


## ORIGINAL ARTICLE

# A long non-coding RNA (Lrap) modulates brain gene expression and levels of alcohol consumption in rats

Laura M. Saba<sup>1</sup> | Paula L. Hoffman<sup>1,2</sup> | Gregg E. Homanics<sup>3</sup> | Spencer Mahaffey<sup>1</sup> | Swapna Vidhur Daulatabad<sup>4</sup> | Sarath Chandra Janga<sup>4,5,6</sup> | Boris Tabakoff<sup>1</sup> 

<sup>1</sup>Department of Pharmaceutical Sciences, Skaggs School of Pharmacy & Pharmaceutical Sciences, University of Colorado Anschutz Medical Campus, Aurora, Colorado, USA

<sup>2</sup>Department of Pharmacology, School of Medicine, University of Colorado Anschutz Medical Campus, Aurora, Colorado, USA

<sup>3</sup>Departments of Anesthesiology, Neurobiology and Pharmacology & Chemical Biology, University of Pittsburgh, Pittsburgh, Pennsylvania, USA

<sup>4</sup>Department of BioHealth Informatics, Indiana University School of Informatics and Computing, Indiana University–Purdue University Indianapolis, Indianapolis, Indiana, USA

<sup>5</sup>Department of Medical and Molecular Genetics, Indiana University School of Medicine, Indianapolis, Indiana, USA

<sup>6</sup>Center for Computational Biology and Bioinformatics, Indiana University School of Medicine, Indianapolis, Indiana, USA

## Correspondence

Boris Tabakoff, Department of Pharmaceutical Sciences, Skaggs School of Pharmacy & Pharmaceutical Sciences, University of Colorado Anschutz Medical Campus, 12850 E. Montview Blvd., Aurora, CO 80045.  
Email: boris.tabakoff@cuanschutz.edu

## Funding information

Banbury Fund; Ethanol Mechanisms in GABAAR gene targeted mice, Grant/Award Number: R37AA010422; Mapping RNA Protein Interaction Networks in the Human Genome, Grant/Award Number: R01GM123314; Overall NIDA Core "Center of Excellence" in Transcriptomics, Systems Genetics and the Addictome, Grant/Award Number: P30DA044223; Role of noncoding RNA in Alcohol Action, Grant/Award Number: U01AA020889; The Heritable Transcriptome and Alcoholism, Grant/Award Number: R24AA013162

## Abstract

LncRNAs are important regulators of quantitative and qualitative features of the transcriptome. We have used QTL and other statistical analyses to identify a gene coexpression module associated with alcohol consumption. The "hub gene" of this module, Lrap (Long non-coding RNA for alcohol preference), was an unannotated transcript resembling a lncRNA. We used partial correlation analyses to establish that Lrap is a major contributor to the integrity of the coexpression module. Using CRISPR/Cas9 technology, we disrupted an exon of Lrap in Wistar rats. Measures of alcohol consumption in wild type, heterozygous and knockout rats showed that disruption of Lrap produced increases in alcohol consumption/alcohol preference. The disruption of Lrap also produced changes in expression of over 700 other transcripts. Furthermore, it became apparent that Lrap may have a function in alternative splicing of the affected transcripts. The GO category of "Response to Ethanol" emerged as one of the top candidates in an enrichment analysis of the differentially expressed transcripts. We validate the role of Lrap as a mediator of alcohol consumption by rats, and also implicate Lrap as a modifier of the expression and splicing of a large number of brain transcripts. A defined subset of these transcripts significantly impacts alcohol

**Abbreviations:** A3SS, alternative 3' splice site; A5SS, alternative 5' splice site; API, application programming interface; AS, alternative splicing; BN, Brown Norway; CNS, central nervous system; Ct, cycle threshold; DE, differentially expressed; FDR, false discovery rate; GO, gene ontology; HISAT2, hierarchical indexing for spliced alignment of transcripts 2; KEGG, Kyoto Encyclopedia of Genes and Genomes; lncRNA, long non-coding RNA; LOD, logarithm of the odds; Lrap, long non-coding RNA for alcohol preference; MXE, mutually exclusive exons; ORF, open reading frame; PCR, polymerase chain reaction; qRT-PCR, quantitative real-time polymerase chain reaction; QTL, quantitative trait loci; RetI, retained intron; RI, recombinant inbred; rMATS, replicate multivariate analysis of transcript splicing; RNASeq, RNA sequencing; RSEM, RNA-seq by expectation-maximization; SE, skipped exon; sgRNA, single guide RNA; SHR, spontaneously hypertensive rat; SNP, single nucleotide polymorphism; SOI, sum of isoforms; WGCNA, weighted gene co-expression network analysis.

[Correction added on 22 October 2020, after first online publication: The article category has been updated from "Review" to "Original Article" in this current version.]

This is an open access article under the terms of the Creative Commons Attribution-NonCommercial-NoDerivs License, which permits use and distribution in any medium, provided the original work is properly cited, the use is non-commercial and no modifications or adaptations are made.

© 2020 The Authors. Genes, Brain and Behavior published by International Behavioural and Neural Genetics Society and John Wiley & Sons Ltd.

consumption by rats (and possibly humans). Our work shows the pleiotropic nature of non-coding elements of the genome, the power of network analysis in identifying the critical elements influencing phenotypes, and the fact that not all changes produced by genetic editing are critical for the concomitant changes in phenotype.

#### KEYWORDS

brain RNA expression networks, long non-coding RNA, predisposing factors, genetic modification, CRISPR/Cas, quantitative genetics, recombinant inbred rat strains, systems genetics, transcriptome, voluntary alcohol consumption

## 1 | INTRODUCTION

Long non-coding RNA (lncRNA) is a class of transcribed elements that is present in living cells from an organism's conception to death.<sup>1,2</sup> These >200 bp transcripts have been shown to influence transcription, translation and splicing events,<sup>3-5</sup> and to play a critical role in the development and senescence of an organism.<sup>6,7</sup> During adulthood, the mammalian brain has the largest assortment of lncRNAs, compared with other organs, and several have been shown to participate in neuronal and glial function.<sup>8,9</sup>

Alcohol (ethanol) consumption is evident in phyla from insects (*Drosophila*)<sup>10</sup> to mammals (including *Homo sapiens*). Alcohol is consumed for a number of reasons, including being a source of calories, for gustatory reward, and for its psychoactive properties.<sup>11,12</sup> The consumption of alcohol is also a sine qua non for development of alcohol addiction (Alcohol Use Disorder), and both alcohol consumption and Alcohol Use Disorder have been shown to have a major genetic component.<sup>13</sup>

In exploring the genetic and neural determinants of levels of alcohol consumption by animals, we previously applied a series of systems genetics analyses to microarray data that included measures of brain RNA expression levels across a panel of recombinant inbred (RI) and selectively bred rats that differed significantly in their levels of voluntary alcohol consumption.<sup>14</sup> Our results identified a gene co-expression module, consisting of 17 gene products, that was implicated in influencing the levels of alcohol consumption. The "hub gene" of the module (the most connected transcript within the module) was identified as an unannotated transcript that showed all of the characteristics of an lncRNA, and we refer to this transcript as Lrap (Long non-coding RNA for alcohol preference).

We now extend our work by determining, through statistical analysis, whether the expression of one of the genes in the module influences the association between other genes in the module.<sup>15</sup> Based on the results of this analysis we find that the "hub gene" of the module, Lrap, is critical for cohesion of the co-expression module. We generate further information on the sequence of Lrap and illustrate its presence in mouse and human as well as rat.

We then produce rats that are genetically modified by deletion of a portion of the Lrap gene using CRISPR/Cas9 techniques. Using these animals and their wild type controls, we show that this genomic deletion produces a significant change in the quantity of alcohol consumption in a two-bottle choice paradigm. We show that disruption of Lrap produces correlated changes in expression of another

transcript that is a member of the module for which Lrap is the "hub gene", and also produces broad changes in expression and splicing of other transcripts in brain. In all, we show that the constitutive disruption of the Lrap gene sequence produces a broad spectrum of changes in brain gene expression, and that subsets of the Lrap-affected transcriptional events can significantly alter alcohol consumption.

## 2 | MATERIALS AND METHODS

All procedures involving animals were approved by the Institutional Animal Care and Use Committee of the University of Pittsburgh or the Institutional Animal Care and Use Committee of the University of Colorado Anschutz Medical Campus and were performed in accordance with the guidelines in the NIH Guide for the Care and Use of Laboratory Animals.

### 2.1 | Identification of transcripts responsible for network cohesiveness

To prioritize which transcript should be disrupted within the previously-identified candidate module for alcohol consumption,<sup>14</sup> we assessed the individual association (correlation) of each transcript with alcohol consumption, and the association of the expression levels of each transcript with the alcohol consumption QTL on rat chromosome 12.<sup>14</sup> We also evaluated each transcript's connectivity within the module, and the changes in network cohesion when we "mimicked" a scenario where the expression level of one of the transcripts does not vary among samples (partial correlation analysis).

#### 2.1.1 | Use of data from previously published work for further analysis

##### *Gene expression analysis*

Expressed transcripts were identified and their expression was quantitated (log base 2), by use of the exon-specific probes on Affymetrix Rat Exon Arrays.<sup>14</sup> In the current work, the individual association of each transcript in the module with alcohol consumption was assessed using Pearson correlation.

### Measurement of alcohol consumption in RI rats

The alcohol consumption values were the measured average daily alcohol consumption by animals of a particular recombinant inbred strain during the second week of a two-bottle choice paradigm.<sup>14</sup> The alcohol consumption for each animal was expressed in grams of alcohol per kilogram of body weight.<sup>14</sup>

### QTL analysis and genetic association analysis

The alcohol consumption QTL that was originally shown to be associated with the candidate brain coexpression module is located on chromosome 12.<sup>14</sup> In the current work, the SNP with the highest LOD score in the genetic region of the alcohol consumption QTL was used to represent the QTL in an association with individual transcript expression levels. Associations were determined using a Welch 2-sample *t* test that assumes unequal variances. For this test, the mean expression level of strains with the BN-Lx genotype at that marker was compared with the mean expression level of strains with the SHR genotype at that marker. Association of individual transcript expression levels with the candidate module eigengene were evaluated using Pearson correlation.

## 2.1.2 | Current work

### Intramodular connectivity analysis to ascertain a target for genetic disruption

Intramodular connectivity was calculated in two ways. First, it was defined for an individual transcript as the sum of the absolute value of its correlation coefficients with all other transcripts within the module. Second, it was defined for an individual transcript as the sum of its topological overlap with each other transcript within the module. Topological overlap values are described as part of the weighted gene co-expression network analysis (WGCNA)<sup>16</sup> and are derived by first transforming pairwise correlation coefficients to reflect a scale-free network and then quantitating both direct and indirect associations between a pair of transcripts.

### Assessment of module cohesion

To examine the influence of an individual transcript, or the module eigengene QTL, on module cohesion, we compared the number of edges among the other transcripts in the module to the number of edges that remain in an 'adjusted' module after controlling for the effect of the transcript or QTL. For this analysis, an edge in the original module is defined as a correlation coefficient with an absolute value greater than 0.30. An edge that is retained in the 'adjusted' network is defined as a partial correlation coefficient with an absolute value greater than 0.30. In the context of the transcript effect, partial correlation is used to examine the association between expression levels of two transcripts after accounting for the variation in both transcripts that may be due to a "third" transcript. A large decrease in the number of edges between the original and the adjusted networks may indicate that the "third" transcript influences the relationships among other transcripts in the module, and that

eliminating the variation in expression of this transcript disrupts the network structure.

## 2.2 | Molecular disruption of Lrap

### 2.2.1 | sgRNA/Cas9 production

CRISPR/Cas9 was used to create Lrap knockout (–/–) rats using techniques previously described.<sup>17,18</sup> Briefly, two sgRNAs targeting Lrap in exon 3 surrounding a suspected open reading frame<sup>14</sup> were identified using the CRISPR Design Tool.<sup>19</sup> sgRNA#1 was designed to cut Lrap immediately 5' of the putative start codon. This sgRNA was created from 2 overlapping PCR primers (F:GAAATTAATACGACTCAC TATAGGCTGTCTCCACATCTTTGGCGTTTTAGAGCTAGAAATAGC; R:AAAAGCACCGACTCGGTGCCACTTTTTCAAGTTGATAACGGACT AGCCTTATTTAACTTGCTATTTCTAGCTCTAAAAC) to generate a T7 promoter-containing sgRNA template as described.<sup>20</sup> sgRNA#2 was designed to cut immediately downstream of the putative translation termination codon. This sgRNA was similarly created using the same reverse primer described above and an overlapping forward primer (GAAATTAATACGACTCACTAT AGGAGCCCTTTGTGAGCA TATGTTTTAGAGCTAGAAATAGC). These templates were transcribed in vitro from the T7 promoter using a MEGashortscript Kit (Ambion/Thermo Fisher Scientific, Austin, TX). The Cas9 coding sequence was amplified from pX330<sup>21</sup> using a T7 promoter-containing forward primer (tattacgactcactataggGAGAATGGACTATAAGGACCACGAC) and reverse primer (GCGAGCTCTAGGAATTCTTAC) and subcloned into pCR2.1-TOPO. This plasmid was linearized with EcoRI, in vitro transcribed and polyA tailed using the mMessage mMachine T7 Ultra Kit (Ambion). Following synthesis, the sgRNAs and Cas9 mRNA were purified using the MEGAclear Kit (Ambion), ethanol precipitated, and resuspended in DEPC-treated water.

### 2.2.2 | Rat production

sgRNAs (25 ng/μl each) and Cas9 mRNA (50 ng/μl) were combined in embryo injection buffer (10 mM Tris, pH 7.4, 0.1 mM EDTA), aliquoted, and stored at –80° C until use. Wistar (Charles River, Wilmington, MA) one-cell embryos were collected from superovulated females and cultured in KSOM media (Sigma-Aldrich, St. Louis, MO) at 37° C in 5% CO<sub>2</sub>/95% air. Embryos were briefly transferred to M2 medium and the nucleic acid mixture was injected into cytoplasm. Embryos that survived injection were transferred to the oviduct of day 0.5 postcoitum pseudopregnant Long Evans (Charles River, Wilmington, MA) recipient females.

### 2.2.3 | Rat genotype analysis

Pups resulting from injected embryos were screened for DNA sequence changes in exon 3 of the Lrap gene by PCR/DNA sequence

analysis. Briefly, a crude DNA extract was prepared from rat tail tips or ear punches using 150  $\mu$ l QuickExtract (Epicenter, Madison, WI). An 846 bp amplicon (+/+) from exon 3 was PCR amplified with forward (Lrap F1: GCTGTCAGAACACAGACCCA) and reverse (Lrap R1: GGAATCTGGCTGGGAAACA) primers. PCR products were sequenced directly or subcloned into pCR2.1-TOPO (Invitrogen) and sequenced. For routine genotyping, PCR products were analyzed on 2% agarose in TAE buffer.

Because a naturally occurring polymorphism that creates a premature stop codon in the *Grm2* gene is present in commercially available Wistar rats, and this polymorphism has been reported to influence the alcohol phenotype,<sup>22</sup> rats were also genotyped for this polymorphism. Those rats harboring the premature stop codon were eliminated from the Lrap pedigree.

## 2.2.4 | Off target analysis

The sgRNA target sequences (sgRNA#1: GCCCAAAGATGTGGAGACAG; sgRNA#2: ATATGCTCACAAAAGGGCTC) were run through the Off – Targets tool of the Cas9 Online Designer site (<http://cas9.wicp.net>). The top 8 predicted off targets for each sgRNA were amplified from male Founder rat #5254 DNA and sequenced.

## 2.3 | Quantitative RT-PCR

Quantitative RT-PCR (qRT-PCR) was used to validate the disruption of Lrap in the genetically modified rats, and to assess levels of expression of module transcripts in the wild-type (+/+), Lrap knockout (–/–) and Lrap heterozygous (+/–) rats.

### 2.3.1 | RNA isolation, reverse transcription

Rat brain RNA was isolated using an RNeasy Mini Kit with RNA MinElute for RNA cleanup (Qiagen, Germantown, MD). The cDNA first strand transcription was performed in duplicate using 1.5  $\mu$ g of total RNA with the iScript RT mix for qRT-PCR following the manufacturer's protocol (BioRad, Hercules, CA). cDNA was stored at  $-20^{\circ}\text{C}$  until further use.

### 2.3.2 | Primer design for SYBR green

Design for primers that assay various regions of the Lrap sequence were limited to specific regions of sequence unique to each of three exon sequences. Primers were selected using Primer3 (<http://frodo.wi.mit.edu/>) and are described in Reference 14. Primers for *lft81*, *P2rx4* and *Txnip* were obtained from Integrated DNA Technologies

(Coralville IA), and targeted exon 12–13 of *lft81*; exon 2–4 of *P2rx4*; and exon 3–4 of *Txnip*.

### 2.3.3 | Measurement and quantification of RNA expression levels

Quantitative PCR was performed on a Roche LightCycler 480II Real Time PCR instrument, using Roche SYBR Green I Master Mix (Indianapolis, IN). Primers used to determine levels of the full length Lrap transcript spanned exons 1–3 (Exon 1 F2 and Exon 3 R1).<sup>14</sup> To assess levels of other exons, primers were used that spanned exons 1–2 (Exon 1 F2 and Exon 2 R1) or exons 2–3 (Exon 2 F1 and Exon 3 R1).<sup>14</sup> PCR was carried out in a 15  $\mu$ l volume and a final concentration of 1X reaction buffer, 500 nM forward and reverse primers and 0.5  $\mu$ l of cDNA reaction. All standard curve and validation reactions were performed in triplicate with NTC reactions for all primer sets, and all samples were done in duplicate. PCR cycling parameters were as follows: hot-start at  $95^{\circ}\text{C}$  for 5 min, 50 cycles of  $95^{\circ}\text{C}$  for 10 s,  $61^{\circ}\text{C}$  for 20 s,  $72^{\circ}\text{C}$  for 45 s, followed by a dissociation curve measurement from 65 to  $97^{\circ}\text{C}$ . For relative quantification, Advanced Relative Quantification analysis with efficiency correction (standard curves) was performed using the LC480II data collection software release 1.5.0.39. Geometric averaging of three reference genes (*Actb*, *CypA* and *Pgk1*) was used to normalize target gene transcripts. Melt curve analysis for all assays was used to verify single product amplification and absence of primer dimers. NTC reactions for all primer sets were  $>5\text{Cq}$  from samples, except in the case of samples from Lrap<sup>–/–</sup> and/or Lrap<sup>+/-</sup> rats where Lrap was measured.

To calculate absolute amounts of the Lrap transcript, cDNA was amplified from Lrap<sup>+/+</sup> rat brain RNA by PCR, using primers Exon1 F2 and Exon 3 R1,<sup>14</sup> and was purified on a D2500 column (Omega Bio-tek, Life Sciences Products, Frederick, CO). cDNA was quantified by absorbance and diluted to produce a standard curve ( $2.27 \times 10^{-1}$  to  $2.27 \times 10^{-8}$  ng). qRT-PCR was performed (primers Exon 1 F2 and Exon 3 R1)<sup>14</sup> using this cDNA and cDNA from brains of Lrap<sup>+/+</sup>, Lrap<sup>+/-</sup> and Lrap<sup>–/–</sup> rats, as described above. Amounts of transcripts were calculated based on regression analysis of the standard curve.

For the relative quantitation qRT-PCR experiments, differences between genotypes were determined using the  $\Delta\Delta\text{Ct}$  method. Differences in  $\Delta\text{Ct}$  values were estimated using a one-way ANOVA model with post hoc testing using estimated marginal means via the *emmeans* package (version 1.4.8) in R without multiple testing correction. Estimated  $\Delta\Delta\text{Ct}$  values were transformed into relative quantities (i.e.,  $2^{-\Delta\Delta\text{Ct}}$ ) compared with wild type. For the relative quantitation of Lrap, a repeated measures one-way ANOVA was used to account for duplicate assays of individual samples. For absolute quantitation qRT-PCR experiments, values were log base 10 transformed prior to statistical analysis and then subjected to differential expression analysis using a one-way ANOVA model with post hoc testing using marginal means without multiple testing correction.

## 2.4 | Measures of impact of Lrap on alcohol consumption

Male Lrap<sup>+/+</sup>, Lrap<sup>-/-</sup> and Lrap<sup>+/-</sup> rats, 90 days old, were given a choice of 10% alcohol or water, as previously described.<sup>23</sup> Data on alcohol consumption obtained daily during the second and third weeks of 2-bottle choice alcohol consumption were used for statistical analyses (g/kg body weight of alcohol consumed/day). To measure daily “alcohol preference”, we divided the volume of a 10% alcohol solution consumed by the total volume of fluid consumed for each of the tested animals. The (geometric) average of daily alcohol consumption and alcohol preference measures for each week was used in analyses.

A linear mixed model was used to determine the effect of genotype (Lrap<sup>+/+</sup>, Lrap<sup>+/-</sup>, and Lrap<sup>-/-</sup>) on amount of alcohol consumed (log base 2 transformed), alcohol preference (log base 2 transformed), daily fluid consumption in milliliters, and weight of the rat in grams. This model included a random effect to account for multiple measures on the same rat and a heterogeneous covariance structure that allowed for differences in variance between genotypes. Post hoc testing was done using least squares estimates and no multiple testing correction. The Satterthwaite method for estimated degrees of freedom was used for fixed effects testing and post hoc testing. The linear mixed model was executed using the MIXED procedure in SAS Statistical Software (version 9.4; Cary NC).

## 2.5 | Measures of impact of Lrap on the brain transcriptome

To assess global changes in gene expression in response to disruption of the Lrap gene, total RNA was extracted from whole brain of three alcohol-naïve male rats from each of the three genotypes (Lrap<sup>+/+</sup>, Lrap<sup>+/-</sup>, and Lrap<sup>-/-</sup>) using the RNeasy Midi Kit with additional cleanup performed using the RNeasy Mini Kit (Qiagen, Valencia, CA). Sequencing libraries were constructed using the Illumina TruSeq Stranded RNA Library Prep Kit with Ribo-Zero (Illumina, San Diego, CA), in accordance with the manufacturers protocol. This library prep kit includes the removal of ribosomal RNA. Library quality was assessed using the Agilent Bioanalyzer 2100 (Agilent Technologies, Santa Clara, CA). Samples were sequenced (2 × 100 paired-end reads) on the Illumina HiSeq2500 (Illumina, San Diego, CA) with four libraries multiplexed per lane.

The pipeline for the RNASeq analysis and differential expression analysis is described below. Reads were trimmed to remove adapters and low-quality base calls using cutadapt.<sup>24</sup> Trimmed reads were aligned to the rn6 version of the rat genome using HISAT2.<sup>25</sup> A genome- and transcriptome-guided reconstruction was executed using the StringTie software for each genotype independently using the Ensembl rat transcriptome (rn6), and then genotype-specific transcriptomes were merged into a single transcriptome<sup>26</sup> using the *merge* function within StringTie. Transcripts were annotated by comparing

the merged transcriptome back to the Ensembl rat transcriptome (rn6) using 'gffcompare'.<sup>27</sup>

For quantitating RNA expression levels, expression can be either estimated for individual isoforms (i.e., splice variants) or estimated as the sum of expression across all isoforms that map to a given gene, that is, sum of isoforms (SOI). In the expression analyses presented here, RNA expression estimates were derived separately, at both the isoform-level and at the SOI-level, and were analyzed separately. This was done to ensure the capture of all relevant information, particularly since lncRNA has been shown to affect transcript splicing,<sup>4,28</sup> and a change in the ratio of isoforms may be missed if only the total of all isoforms expressed from a gene was considered.

Individual isoforms and SOIs from the merged transcriptome were quantitated using RSEM.<sup>29</sup> Transcripts were tested for differential expression using the DESeq2 package in R.<sup>30</sup> A false discovery rate (FDR) was used to account for multiple testing.<sup>31</sup> Isoforms and SOIs were only included in these analyses if they could be annotated as a product of a protein-coding gene (Ensembl annotated isoforms and novel isoforms associated with Ensembl annotated genes) and if the sum of the estimated read counts across all samples from the Lrap<sup>-/-</sup> and Lrap<sup>+/+</sup> animals was greater than 50.

Genes were included in a functional enrichment analysis if their isoform or SOI expression levels were significantly different between Lrap<sup>+/+</sup> and Lrap<sup>-/-</sup> rats (FDR < 0.10). Functional enrichment of KEGG pathways<sup>32</sup> and Gene Ontology (GO<sup>33</sup>;) categories was determined using a Fisher's exact test where the background gene list only included genes with at least one isoform or SOI expressed in rat brain (total estimated read counts across six samples from the Lrap<sup>-/-</sup> and Lrap<sup>+/+</sup> animals was greater than 50). KEGG annotation was retrieved using the KEGG API (<sup>32</sup>; Release 88.0) and GO annotation was retrieved using the 'biomaRt' package in R (<sup>34</sup>; Ensembl Gene 94; version 2.36.1). Programs related to the RNA-Seq analysis are available at <http://github.com/SabaLab/LrapKO>. The raw RNA-Seq data are available through GEO (GSE1557079) and the processed data are available on PhenoGen (<http://phenogen.org>).

## 2.6 | Identification of Lrap-influenced transcripts associated with alcohol consumption

To further focus attention on the differentially expressed transcripts with a higher probability of being associated with the Lrap-induced differences in alcohol consumption between the Lrap<sup>-/-</sup> and Lrap<sup>+/+</sup> rats, we established three criteria for inclusion of the information from both the genetically manipulated rats and from the RI panel.<sup>14</sup> First, the SOI for a given gene had to be differentially expressed between Lrap<sup>+/+</sup> and Lrap<sup>-/-</sup> rats (unadjusted *p* value <0.05). Second, the transcript levels of a gene (derived from microarray analysis) had to be significantly (Pearson correlation coefficient, unadjusted *p* value <0.05) correlated with alcohol consumption in the HXB/BXH RI panel. Finally, the transcript levels of a

gene had to be correlated with *Lrap* expression (Pearson correlation coefficient, unadjusted *p* value <0.05) in the HXB/BXH RI panel.

## 2.7 | Analysis of differential alternative splicing

RNASeq data provides an opportunity to detect differential alternative splicing events across conditions. Employing the replicates of RNASeq data across pairs of conditions (i.e., *Lrap*<sup>+/+</sup> vs. *Lrap*<sup>-/-</sup> rats), we applied rMATS (replicate Multivariate Analysis of Transcript Splicing)<sup>35</sup> to identify differential alternative splicing (AS) events. rMATS provides a computational framework to identify all possible splicing events which are altered between two samples, by inspecting the status of exons/introns as they are included or excluded resulting from alternative splicing. We used sorted BAM (Binary Alignment/Map) files, obtained from aligning the raw RNASeq datasets against the rat reference genome using HISAT,<sup>25</sup> as input to rMATS. *Lrap*<sup>+/+</sup> and *Lrap*<sup>-/-</sup> rats were examined for alterations in various splicing events. We have provided the reconstructed brain transcriptome as described above as input to rMATS and have used the default thresholds for remaining options. Briefly, rMATS enabled us to analyze the inclusion/exclusion of target exons/introns contributing to different types of alternative splicing events, namely skipped exon (SE), alternative 5' splice site (A5SS), alternative 3' splice site (A3SS), mutually exclusive exons (MXE) and retained intron (Rel), across any pair of conditions with replicates. An AS event is quantified based on the difference in the level of inclusion of an exon which is defined as the splice index or percentage spliced index (*ψ score*) between two samples or conditions and ranges between 0 and 1. Significant differences in the values of *ψ* for an exon, between a pair of conditions compared with a null distribution indicate its differential abundance. Alternative splicing events between *Lrap*<sup>+/+</sup> and *Lrap*<sup>-/-</sup> rats for the isoforms that were differentially expressed were examined using reads that span splicing junctions and an FDR threshold of 0.10.

## 2.8 | Informatic characterization of *Lrap*

### 2.8.1 | Homology of *Lrap* across rat, mouse and human

To ascertain the possible presence of sequences similar to the DNA sequence in rat that gives rise to *Lrap*, the reference rat genome sequence for the region containing *Lrap* on the negative strand was obtained from the UCSC genome browser and variants including SNPs and short insertions and deletions were included from the SHR/WKY strains as reported by Hermsen et al.<sup>36</sup> The sequence was submitted to run BLASTN through the Ensembl website (v 98) against the human and mouse genomes, using distant homology search sensitivity with the default settings, except we required a minimum e-value reporting of 1e-3, word size of 7 and gap penalty of 2,2. Aligned blocks were converted to a bed file to include custom alignment

tracks in the UCSC genome browser to generate a browser image for each species.<sup>37</sup>

### 2.8.2 | Overlap of RNA expression in a human cell line with homologous regions

Publicly available RNA sequencing reads from polyA- long RNA were downloaded from the UCSC Genome Browser [72]. These data were derived from the GM12878 cell line and are part of the Long RNASeq from ENCODE/Cold Spring Harbor Lab track (GEO Accession: GSM758572).<sup>8</sup> Reads were aligned to the human genome (hg38 version) using HISAT2.<sup>25</sup> The graphic depicting the RNASeq coverage was generated using the UCSC Genome Browser.<sup>37</sup>

## 3 | RESULTS

### 3.1 | Identification of transcripts responsible for network cohesiveness

Examination of intramodular connectivity of all the transcripts contained in the module in which *Lrap* was identified as a hub gene,<sup>14</sup> indicated that *Lrap* was the most highly connected transcript using either correlation coefficients or topological overlap (connectivity) measures (Table 1). Furthermore, *Lrap* had the largest impact on module integrity/connectivity among all transcripts in the module (Table 1). In fact, more edges (connections) were disrupted when adjusting for *Lrap* than when adjusting for the module eigengene QTL. Theoretically, a connection between the products of two genes that was present (absolute value of the correlation coefficient > 0.3) in the original module, but was eliminated after adjusting for the effect of *Lrap*, represents an indirect association between the expression levels of those two gene products that is due to the influence of *Lrap* on both transcripts. Because of the evidence related to *Lrap*'s central role in the cohesiveness of this module, and the desire to better understand the role of *Lrap* in determining the expression levels of the module transcripts, we chose to disrupt the *Lrap* gene and assess, not only the effects of the disruption on the expression of the transcripts in the module, and transcript levels throughout the brain, but also the effect of disruption on alcohol consumption.

### 3.2 | *Lrap*<sup>-/-</sup> rat production

Two sgRNA sequences were used with the CRISPR/Cas9 system to create a deletion in exon 3 of *Lrap*. The sgRNA sequences were designed based on the genomic sequence of the Brown Norway (BN) rat (Rn6) (Figure 1A). It should be noted that the parental strains of the HXB/BXH RI panel, BN-Lx/Cub and SHR/OlaIpcv, used for our QTL mapping and correlation analysis, are derived from the BN and the Wistar strains, respectively. We ascertained that the chosen sequences were also a perfect match to genomic sequences in the

**TABLE 1** Prioritization of transcripts within the alcohol consumption module for genetic manipulation

Gene symbol	Genomic position	Correlation with alcohol consumption [correlation coefficient (p value)]	Association with alcohol consumption on chromosome 12 [log base 2 difference (p value)]	Correlation with module eigengene [correlation coefficient (p value)]	Correlation-based intramodular connectivity (rank within module)	Connectivity-based intramodular connectivity (rank within module)	Number of connected nodes <sup>a</sup> in module ( correlation coefficient  > 0.3)	Percent of all edges in module that remain after adjustment for transcript
Lrap	chr12: 39.01 Mb	-0.55 (0.011)	-0.32 (0.0079)	0.90 (4.1e-08)	10.66 (1)	2.99 (1)	16	41%
lft81	chr12: 39.42 Mb	-0.43 (0.051)	-0.17 (0.0015)	0.88 (2.0e-07)	10.33 (2)	2.66 (2)	15	49%
Coq5	chr12: 47.08 Mb	-0.50 (0.021)	-0.10 (0.0057)	0.83 (2.6e-06)	9.94 (4)	2.24 (3)	15	65%
Txnip	chr2: 198.68 Mb	0.61 (0.003)	0.20 (0.0087)	-0.77 (4.6e-05)	9.09 (8)	2.20 (4)	13	74%
P2rx4	chr12: 39.31 Mb	-0.63 (0.002)	-0.17 (0.0022)	0.83 (3.6e-06)	9.86 (5)	2.15 (5)	16	62%
Tmem116	chr12: 40.56 Mb	0.34 (0.133)	0.34 (0.0001)	-0.81 (7.5e-06)	9.95 (3)	2.00 (6)	16	49%
Maats1	chr11: 64.98 Mb	-0.56 (0.008)	-0.05 (0.0772)	0.65 (1.3e-03)	7.57 (14)	1.95 (7)	9	95%
GENE_27603	chr6:42.79 Mb	-0.50 (0.021)	-0.12 (0.0298)	0.70 (4.5e-04)	8.18 (11)	1.74 (8)	13	83%
Oas1f (formerly Oas1b)	chr12: 41.26 Mb	0.34 (0.136)	0.61 (0.0006)	-0.79 (2.2e-05)	9.61 (6)	1.69 (9)	16	53%
GENE_18197	chr2:257.76 Mb	-0.40 (0.075)	-0.12 (0.0196)	0.77 (3.9e-05)	9.25 (7)	1.65 (10)	15	68%
Parp3	chr8: 115.17 Mb	-0.28 (0.221)	-0.05 (0.0159)	0.67 (8.0e-04)	8.40 (10)	1.47 (11)	15	76%
GENE_03396	chr1:259.43 Mb	0.27 (0.240)	0.22 (0.0032)	-0.65 (1.4e-03)	7.97 (12)	1.44 (12)	12	72%
Sic8b1 (formerly Sic24a6)	chr12: 41.57 Mb	0.16 (0.496)	0.11 (0.0004)	-0.62 (2.5e-03)	7.60 (13)	1.42 (13)	12	86%
Prkar1b	chr12: 17.61 Mb	0.30 (0.192)	0.07 (0.0721)	-0.68 (7.6e-04)	8.44 (9)	1.41 (14)	15	72%
GENE_04887_ISO_01	chr10:21.98 Mb	0.25 (0.266)	0.08 (0.0113)	-0.49 (2.3e-02)	6.46 (16)	1.28 (15)	9	87%
Pcdhb5	chr18: 30.40 Mb	-0.10 (0.668)	-0.06 (0.0497)	0.54 (1.2e-02)	6.92 (15)	1.25 (16)	10	82%
Anxa11	chr16: 3.87 Mb	0.25 (0.271)	0.02 (0.3611)	-0.50 (2.0e-02)	6.29 (17)	1.05 (17)	12	92%

Note: Gene symbols that begin with 'GENE' are unannotated transcripts that were identified in the original transcriptome reconstruction. All correlation coefficients are based on a parametric Pearson correlation. None of the p values have been adjusted for multiple testing.

<sup>a</sup>Nodes refer to transcripts in the module.

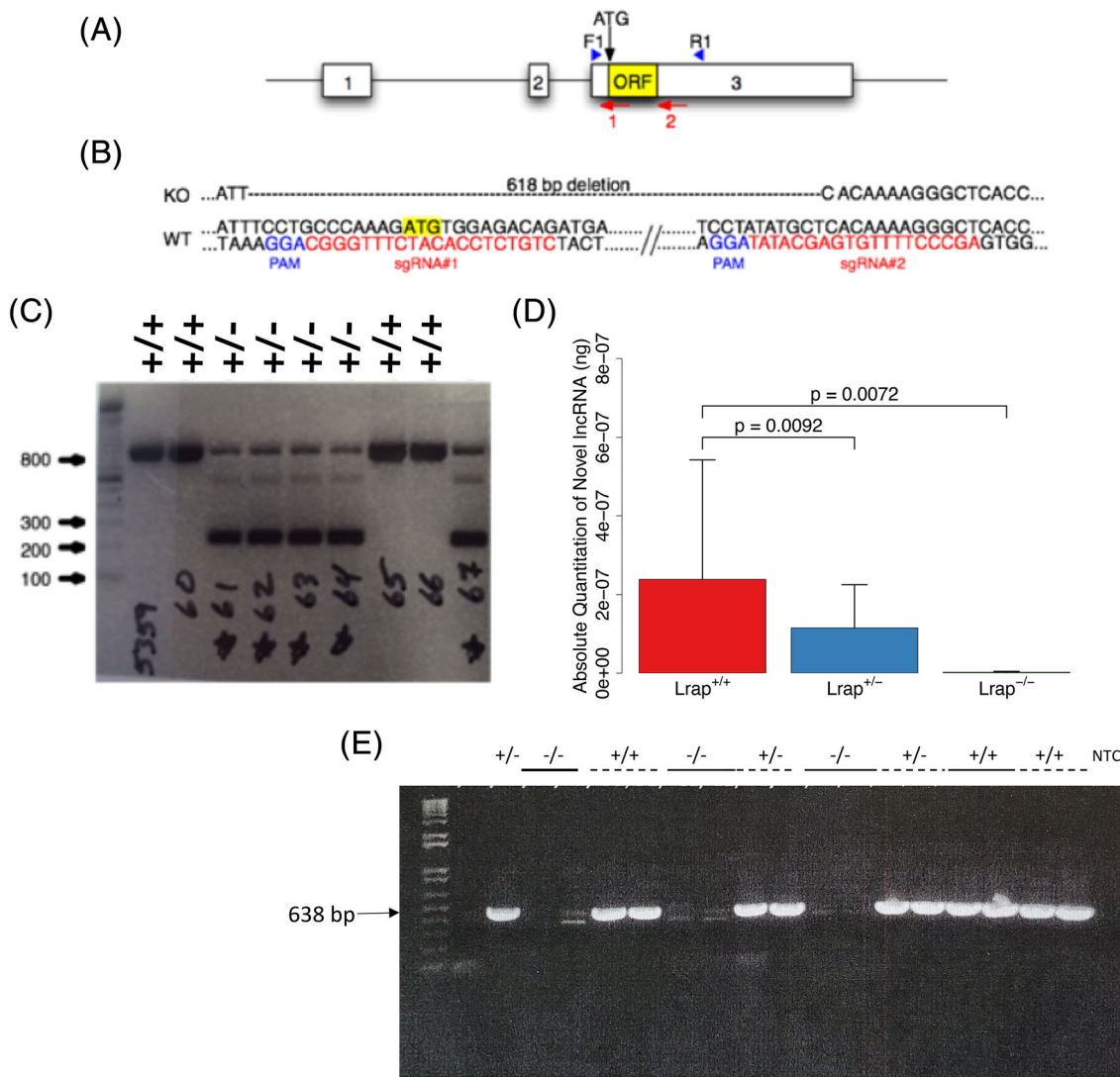


**FIGURE 1**  $Lrap^{-/-}$  rat strategy and characterization. (A) Diagram of  $Lrap$  locus illustrating exons (numbered white boxes), the potential open reading frame (yellow ORF box), the putative start codon (ATG), sgRNA target sites (numbered red arrows) and the location of the forward and reverse PCR genotyping primers (blue arrowheads). (B) Partial  $Lrap$  wild type ( $Lrap^{+/+}$ ) and knockout ( $Lrap^{-/-}$ ) rat genomic DNA sequence. In red are the sgRNA target sequences used for CRISPR/Cas9 gene targeting. The CRISPR protospacer adjacent motifs (PAM) are shown in blue. The yellow highlighted ATG is the putative start codon. Note that the  $Lrap^{-/-}$  sequence harbors a 618 bp deletion. (C)  $Lrap$  PCR genotype analysis. Ethidium bromide stained agarose gel of  $Lrap$  PCR products from  $Lrap$  wild type ( $Lrap^{+/+}$ ) and  $Lrap^{+/-}$  rats. Ladder is in bp. (D) Validation of differences in  $Lrap$  RNA expression using qRT-PCR. RNA expression levels of exons 1–3 in rat brains are reported as absolute quantity ( $n = 3$ /genotype). This PCR product is undetectable in the  $Lrap^{-/-}$  rats, since the exon 3 primer (Exon 3 R1) targets the excised region of exon 3.<sup>14</sup> All statistical analyses were done on the log transformed data and results are reported based on the back transformation of mean values and mean values plus one standard error. All  $p$  values were calculated using a one-way ANOVA with post hoc pairwise comparisons. (E) qRT-PCR products from  $Lrap^{+/+}$ ,  $Lrap^{+/-}$  and  $Lrap^{-/-}$  rats. Ethidium bromide stained agarose gel of products from qRT-PCR of naïve  $Lrap^{+/+}$ ,  $Lrap^{+/-}$  and  $Lrap^{-/-}$  rats, using primers for exons 1 and 3: Exon 1 F2-Exon 3 R1.<sup>14</sup> With the exception of the first lane ( $+/+$ ), all other samples are run as duplicates

same location in the Wistar rat genome. PCR/DNA sequence analysis of 9 founders derived from injected embryos of Wistar rats revealed that 2 were wild type ( $Lrap^{+/+}$ ), 3 had small deletions at one or both sgRNA binding sites, and 4 had deletions spanning the area between the sgRNA binding sites.

Two of the Wistar founders with the large deletions were mated to Wistar females to establish germline transmission, but only one of these produced germline transmission. Founder rat #5254 (aka 4B.3)

appeared heterozygous for a 618 bp deletion (Figure 1B) within which was contained a 2 bp deletion/3 bp insertion (indels) near sgRNA#1 binding site when compared with the BN genome in this region (not shown). All offspring from this founder were genotyped for the 618 bp deletion using the PCR analysis illustrated in Figure 1C. From 27 offspring, 16 were heterozygous for the wild type ( $Lrap^{+/+}$ ) and 618 bp deletion alleles. Note that the  $Lrap^{+/+}$  allele produces an 846 bp fragment whereas the knockout allele ( $Lrap^{-/-}$ ) produces a



228 bp fragment. The PCR amplicons from all heterozygous F1 animals that were shipped for breeding to the University of Colorado were sequenced to verify the fidelity of the mutated locus.

Analysis of the predicted top 8 off-target mutation sites for each sgRNA in Founder rat #5254 revealed no off-target mutations.

### 3.3 | $Lrap^{-/-}$ rat characterization

Rats were bred at the University of Colorado and genotyped by Transnetyx (Cordova, TN). As shown in Figure 1D,E, the absolute quantification of the *Lrap* transcript by qRT-PCR, measured using primers that spanned the full length *Lrap* transcript (exons 1–3, with the reverse primer aligning to the exon 3 deleted region), indicated that there was a significant effect of genotype ( $F_{2,5} = 12.49$ ;  $p = 0.011$ ). More specifically, *Lrap* was significantly decreased in male  $Lrap^{+/-}$  rats ( $p = 0.0092$ ) and not detectable in brains of male  $Lrap^{-/-}$  rats. qRT-PCR was also used to determine relative levels of the *Lrap* transcript in the wild type ( $Lrap^{+/+}$ ),  $Lrap^{+/-}$  and  $Lrap^{-/-}$  rats, using the primers spanning exons 1–3, and similar results were found. Relative transcript levels were also reduced for  $Lrap^{-/-}$  rats (relative expression compared with  $Lrap^{+/+} = 0.002$ ;  $p$  value =  $2.8 \times 10^{-5}$ ) when qRT-PCR was performed using primers spanning exons 2–3 (using the reverse primer targeting the deleted region of exon 3).<sup>14</sup> The reduction in  $Lrap^{+/-}$  rats from the area spanning exons 2–3 was suggestive (relative expression compared with  $Lrap^{+/+} = 0.31$ ;  $p$  value = 0.061). When primers spanning exons 1–2 were used,<sup>14</sup> transcript levels were also reduced but to a lesser extent ( $Lrap^{-/-}$  relative to  $Lrap^{+/+} = 0.16$ ,  $p$  value = 0.041;  $Lrap^{+/-}$  relative to  $Lrap^{+/+} = 0.56$ ,  $p$  value = 0.48).

### 3.4 | Effect of disruption of *Lrap* on alcohol drinking behavior

Because the original candidate coexpression module was identified from correlations/associations with alcohol consumption in a two-bottle choice paradigm with 24-h access to a 10% ethanol solution,<sup>14</sup> an identical phenotype was measured in the genetically manipulated rats. There was a suggestive effect of genotype on alcohol consumption ( $F_{2,22.2} = 3.19$ ;  $p = 0.061$ ). Male  $Lrap^{+/+}$  (Wistar) rats drank an average of 1.1 g of alcohol/kg of body weight/day (Figure 2A). In the  $Lrap^{-/-}$  rats, alcohol consumption was significantly increased to 2.1 g/kg/day (range 0.7–4.4 g/kg/day,  $p = 0.021$ ). The increase in alcohol consumption is consistent with our finding that the expression level of *Lrap* in brains of the HXB/BXH RI rats was negatively correlated with amount of alcohol consumed (Table 1). In the  $Lrap^{+/-}$  rats, alcohol consumption was increased to 1.5 g/kg/day, and this intermediate value was not significantly different from the level observed in the  $Lrap^{-/-}$  rats ( $p = 0.26$ ) or the level observed in the  $Lrap^{+/+}$  rats ( $p = 0.28$ ). When we calculated “alcohol preference” for the  $Lrap^{+/+}$ ,  $Lrap^{+/-}$  and  $Lrap^{-/-}$  rats, the alcohol preference ratio for the  $Lrap^{+/+}$  rats averaged 0.10, a value indicating that the ethanol solution was

aversive to these animals (Figure 2B). There was a significant effect of genotype on alcohol preference ( $F_{2,21.3} = 3.75$ ;  $p = 0.040$ ). The alcohol preference value (0.18) for the  $Lrap^{-/-}$  rats was significantly higher than that for the  $Lrap^{+/+}$  rats ( $p = 0.014$ ) while the alcohol preference ratio for the  $Lrap^{+/-}$  rats fell between those two values and was not significantly different from either ( $p = 0.16$  compared with  $Lrap^{+/+}$  and  $p = 0.29$  compared with  $Lrap^{-/-}$ ). Group average total fluid intake was not significantly different among the  $Lrap^{+/+}$ ,  $Lrap^{+/-}$  and  $Lrap^{-/-}$  animals (Figure 2C;  $F_{2,19.6} = 0.21$ ;  $p = 0.81$ ). Body weight did not differ significantly among the three genotype groups (Figure 2D;  $F_{2,17} = 0.06$ ;  $p = 0.94$ ).

### 3.5 | Effect of disruption of *Lrap* on brain gene expression (RNASeq)

#### 3.5.1 | Global brain gene expression levels in male $Lrap^{+/+}$ , $Lrap^{+/-}$ and $Lrap^{-/-}$ rats

On average, 54 million paired end reads were sequenced per single brain sample (range 36.6–61.4 million) with three individual brain samples per genotype. Of those, between 85% and 95% of reads per sample aligned to the Rn6 version of the rat genome. The merged reconstructed transcriptome included 145,807 isoforms (both polyadenylated and non-polyadenylated) representing 114,700 gene products. Novel isoforms were annotated to an Ensembl protein-coding gene if they shared at least one exon junction with an annotated isoform of an Ensembl protein-coding gene. Of the 38,988 transcript isoforms annotated to a protein-coding gene, 33,063 had expression levels above our pre-determined background (more than 50 total reads from  $Lrap^{-/-}$  and  $Lrap^{+/+}$  rats). The 33,063 isoforms that were expressed above the background, could be assigned to 14,114 protein-coding Ensembl genes. All nine libraries passed quality control standards based on (1) number of reads sequenced (>10 million), (2) percent of reads eliminated during trimming (<10%), (3) percent of reads aligning to the genome (>80% of trimmed reads), and (4) percent of reads aligned to transcriptome (>60% of trimmed reads).

For protein-coding genes which were the source of more than one isoform, the total number of reads that mapped to all the isoforms were summed (Sum Of Isoforms), and these values were subjected to a separate statistical analysis. The process of quantifying both individual isoforms and the composite of all isoforms (SOI) derived from a single gene was predicated on the known function of certain lncRNAs as modulators of alternative splicing.<sup>38</sup>

At an FDR threshold of 0.10, 782 isoforms were differentially expressed (DE) between brains of  $Lrap^{-/-}$  and  $Lrap^{+/+}$  rats. An independent analysis showed that 72 SOIs were differentially expressed when one summed all the reads that could be assigned to each gene and compared the means of these summed reads between the  $Lrap^{-/-}$  and  $Lrap^{+/+}$  rats. The total of the differentially expressed isoforms and total gene products (SOIs) amounted to 750 products of annotated protein coding genes (i.e., some of differentially expressed isoforms

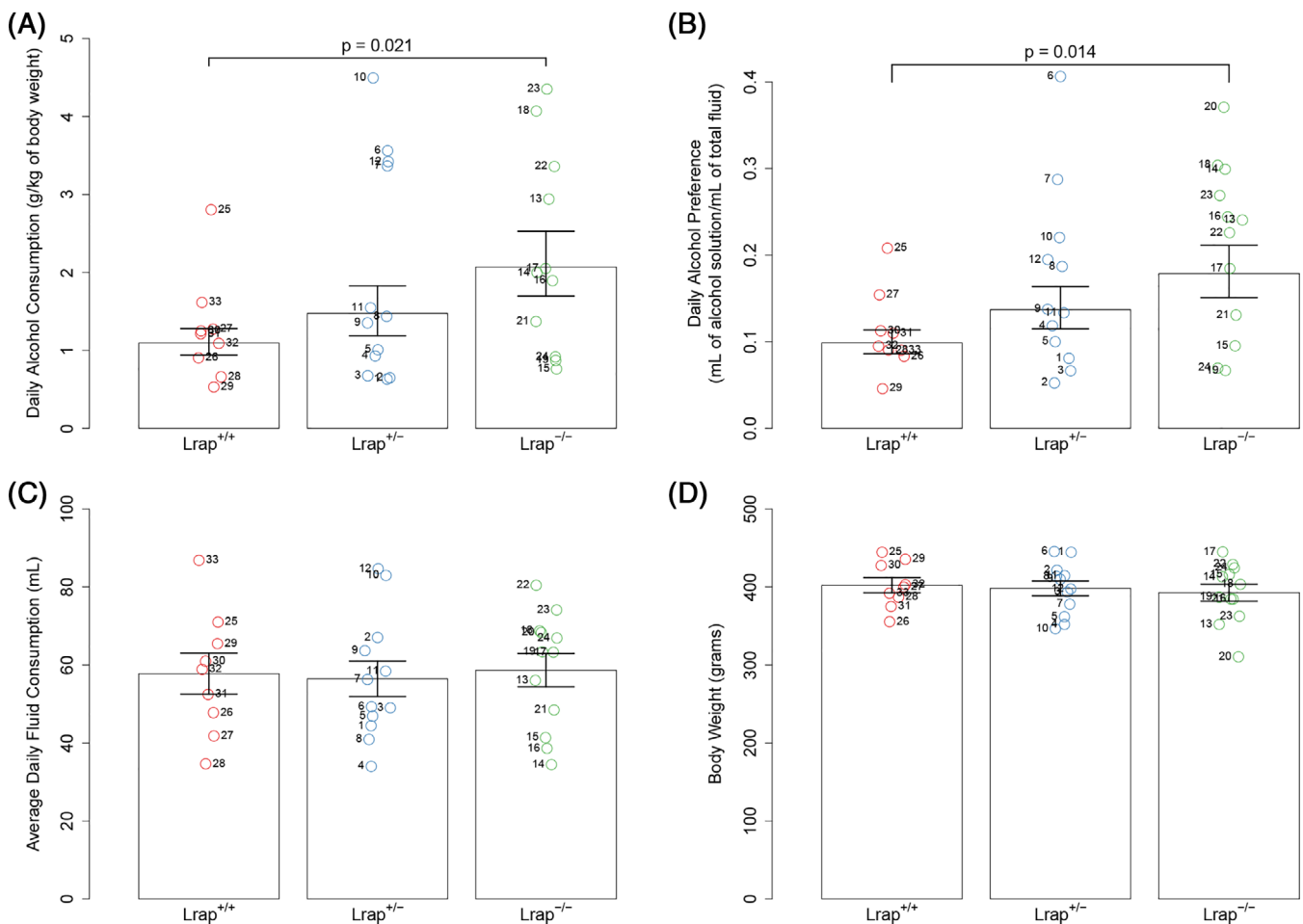


**FIGURE 2** Effect of *Lrap* on alcohol consumption in genetically modified rats. Alcohol consumption by male rats ( $n = 9$ – $12$  rats/genotype) from the three genotypes (*Lrap*<sup>+/+</sup>, *Lrap*<sup>+/-</sup>, and *Lrap*<sup>-/-</sup>) was determined using the two-bottle choice paradigm with 10% ethanol solution. Circles represent values for individual rats. Each point is labeled with a number to facilitate access to raw data if needed. For alcohol consumption and alcohol preference, means  $\pm 1$  standard error from the linear mixed model on log transformed values were transformed back to the original scale and reported in the graphic. For all four outcomes, post hoc pairwise comparisons were made between all three groups and only comparisons with a  $p$  value less than 0.05 are reported. (A) Alcohol consumption in grams per kilogram of body weight. (B) Alcohol preference measured as the volume of alcohol solution divided by the total volume of fluids consumed. (C) Average daily fluid consumption in milliliters. No significant ( $p < 0.05$ ) differences among genotypes were found. (D) Body weight in grams. There were no significant differences in body weight ( $p < 0.05$ ) among genotypes

were annotated to the same SOI and/or for some isoforms, the SOI was also significantly, differentially, expressed).

To explore differential alternative splicing between *Lrap*<sup>+/+</sup> and *Lrap*<sup>-/-</sup> rats (i.e., isoforms present in one line and not present in the other), we used the rMATS algorithm [73] to specifically examine differences in the number of reads that covered individual alternate splice junctions among the 782 isoforms that were differentially expressed between the *Lrap*<sup>+/+</sup> and *Lrap*<sup>-/-</sup> rats. Of the 782 differentially expressed isoforms, only 601 could be tested in this additional manner, because the remaining isoforms did not meet the minimum sequencing coverage needed for the rMATS algorithm to confidently associate them with one of the alternative splicing event types detected by this software. Overall, 133 of the 601 tested isoforms were associated with at least one novel alternative splicing event ( $FDR < 0.10$ , *Lrap*<sup>+/+</sup> vs. *Lrap*<sup>-/-</sup>). A significant novel alternative

splicing event indicates that the splicing event, e.g., a skipped exon, occurred in one group (*Lrap*<sup>+/+</sup> or *Lrap*<sup>-/-</sup>) but not the other. Skipped Exon (SE), Retained Intron (Rel), and Mutually Exclusive Exon (MXE) were found to be the most prevalent types of significant alternative splicing events detected across the isoforms (103 [77%] out of 133 isoforms had at least one of these three types of splicing events). MXE refers to the situation in which two different exons within a gene coding region, when expressed, can determine the quantity of isoform expressed in *Lrap*<sup>+/+</sup> versus *Lrap*<sup>-/-</sup> rats. This results in a transcript isoform exhibiting expression in one condition (e.g., *Lrap*<sup>+/+</sup>) when the first exon is expressed, while in the second condition (*Lrap*<sup>-/-</sup>), a different exon and its corresponding transcript isoform are expressed. As a result, splicing events, especially SEs and MXEs, would likely influence the protein coding sequence arising from the expressed isoforms. The remaining 468 differentially expressed

isoforms in our study did not meet our statistical criteria for identifying novel alternative splicing events distinguishing *Lrap*<sup>+/+</sup> from *Lrap*<sup>-/-</sup> rats and hence likely reflect differences in expression levels of the same isoforms between the *Lrap*<sup>+/+</sup> and genetically manipulated, *Lrap*<sup>-/-</sup>, rats.

Of the transcripts that were part of the module originally associated with alcohol consumption,<sup>14</sup> only *Lrap* and *P2rx4* transcripts were found to be differentially expressed in brains of *Lrap*<sup>+/+</sup> compared with *Lrap*<sup>-/-</sup> rats in this analysis (Table 2). In the particular case of *P2rx4*, the SOI was significantly different between the *Lrap*<sup>+/+</sup> and *Lrap*<sup>-/-</sup> rats, but the ratio of the two isoforms remained constant in each of the genotypes. This indicated that *Lrap* in this case may be affecting the overall transcription of *P2rx4* rather than changing the levels of alternatively spliced isoforms. Of the 12 annotated genes in the module, one gene, *Pcdhb5*, was not detected in the RNASeq data set. Differential expression results for the remaining 11 annotated genes in the module indicated that they were not differentially expressed between *Lrap*<sup>+/+</sup> and *Lrap*<sup>-/-</sup> rats when measured as the

sum of expression of all isoforms or when examining each isoform separately (Table 2). We also performed qRT-PCR analysis of transcripts of *P2rx4*, *Ift81* and *Txnip*, which were three of the most highly connected genes in the co-expression module associated with alcohol consumption (Figure 3). Similar to the RNASeq results, the levels of expression of *Ift81* and *Txnip* were unchanged in the *Lrap*<sup>+/+</sup> and *Lrap*<sup>-/-</sup> rats ( $F_{2,6} = 0.08$  and  $p = 0.92$ ;  $F_{2,6} = 0.51$  and  $p = 0.63$ , respectively), while decreases were indicated in the expression of *P2rx4* in both *Lrap*<sup>+/+</sup> and *Lrap*<sup>-/-</sup> rats ( $F_{2,6} = 3.93$  and  $p = 0.08$ ).

### 3.6 | Informatics analysis of functional correlates of *Lrap* sensitive transcripts

To examine functional enrichment of the significantly differentially expressed transcripts of protein-coding genes (*Lrap*<sup>+/+</sup> vs. *Lrap*<sup>-/-</sup>, FDR < 0.10), we utilized KEGG pathways and Gene Ontology terms. One KEGG pathway ("Tight Junction") was significantly enriched for

**TABLE 2** RNASeq expression levels of transcripts from the original alcohol consumption module in brains of genetically manipulated rats

Gene symbol	Gene description	SOI-level quantitation						
		Median of normalized read count— <i>Lrap</i> <sup>-/-</sup>	Median of normalized read count— <i>Lrap</i> <sup>+/-</sup>	Median of normalized read count— <i>Lrap</i> <sup>+/+</sup>	Ratio of <i>Lrap</i> <sup>-/-</sup> to <i>Lrap</i> <sup>+/+</sup>	Ratio of <i>Lrap</i> <sup>+/-</sup> to <i>Lrap</i> <sup>+/+</sup>	Unadjusted <i>p</i> value	FDR
Anxa11	annexin A11	1485	1423	1540	0.96	0.92	0.975	0.99
Coq5	coenzyme Q5, methyltransferase	324	309	314	1.03	0.98	0.855	0.96
Ift81	intraflagellar transport 81	324	314	372	0.87	0.84	0.258	0.71
<i>Lrap</i> <sup>a</sup>	long non-coding RNA for alcohol preference	14	40	86	0.16	0.47	1.5E-14	1.80E-11
Maats1	MYCBP-associated, testis expressed 1	91	110	109	0.83	1.01	0.386	0.79
P2rx4	purinergic receptor P2X 4	197	187	280	0.70	0.67	0.006	0.26
Parp3	poly (ADP-ribose) polymerase family, member 3	112	107	110	1.01	0.97	0.694	0.91
Prkar1b	protein kinase cAMP-dependent type 1 regulatory subunit beta	6976	6766	6193	1.13	1.09	0.171	0.63
Slc8b1(formerly Slc24a6)	solute carrier family 8 member B1	97	110	91	1.07	1.21	0.511	0.85
Tmem116	transmembrane protein 116	78	94	81	0.96	1.15	0.960	0.99
Txnip	thioredoxin interacting protein	1441	1575	1291	1.12	1.22	0.816	0.95
Oas1f(formerly Oas1b)	2'-5' oligoadenylate synthetase 1F	44	40	46	0.96	0.88	0.920	0.98

<sup>a</sup>Only the isoform targeted for knockout was included for *Lrap*.

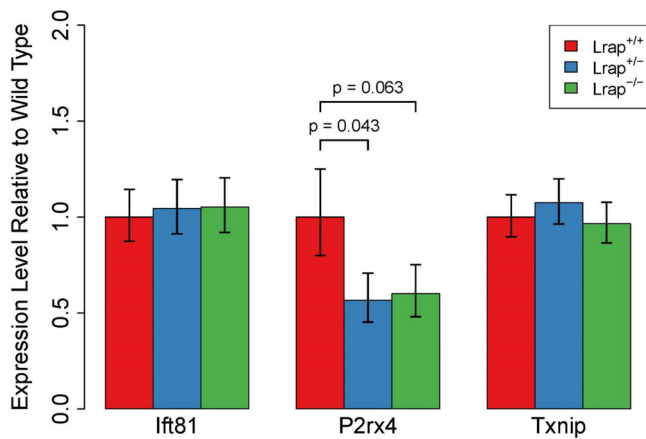


**FIGURE 3** qRT-PCR validation of difference in mRNA expression of genes from the alcohol consumption candidate module. The expression levels of three of the transcripts most highly connected to the hub transcript (*Lrap*) were assessed in brains of alcohol naive male *Lrap* wild type ( $^{+/+}$ ), *Lrap* heterozygous ( $^{+/-}$ ) and *Lrap* knockout ( $^{-/-}$ ) rats ( $n = 3$ ) by qRT-PCR. All statistical analyses were done on the delta Ct data and results are reported based on the transformation of mean values and mean values plus one standard error. All  $p$  values were calculated using a linear model (*lft81*, *P2rx4*, *Txnip*) with post hoc pairwise comparisons

differentially expressed gene products (Figure 4A; criteria: FDR for enrichment  $< 0.10$ ; fold enrichment  $> 2$  and 3 or more differentially expressed genes or isoforms had to be present in a category). This “Tight Junction” pathway (rno04530) contained 19 genes with either an isoform or a SOI that was differentially expressed between *Lrap* $^{-/-}$  and *Lrap* $^{+/+}$  rat brains (Figure 4B). Likewise, 15 GO terms were significantly enriched for genes with either an isoform or a SOI that was differentially expressed (FDR for enrichment  $< 0.10$ ; fold enrichment  $> 2$ , and 3 or more differentially expressed genes/isoforms had to be present in a category). One of the top 5 GO terms was “Response to Ethanol” (GO:0045471). That category contains 15 genes with differentially expressed isoforms or SOIs (Figure 4C). In both the Tight Junction and Response to Ethanol categories it was also noted that the primary differences in expression levels were at the isoform level rather than the SOI (Table S1).

### 3.7 | Identification of *Lrap*-influenced transcripts associated with alcohol consumption

As noted above, there were many isoforms and some SOIs whose RNA expression levels were influenced by the genetic manipulation of

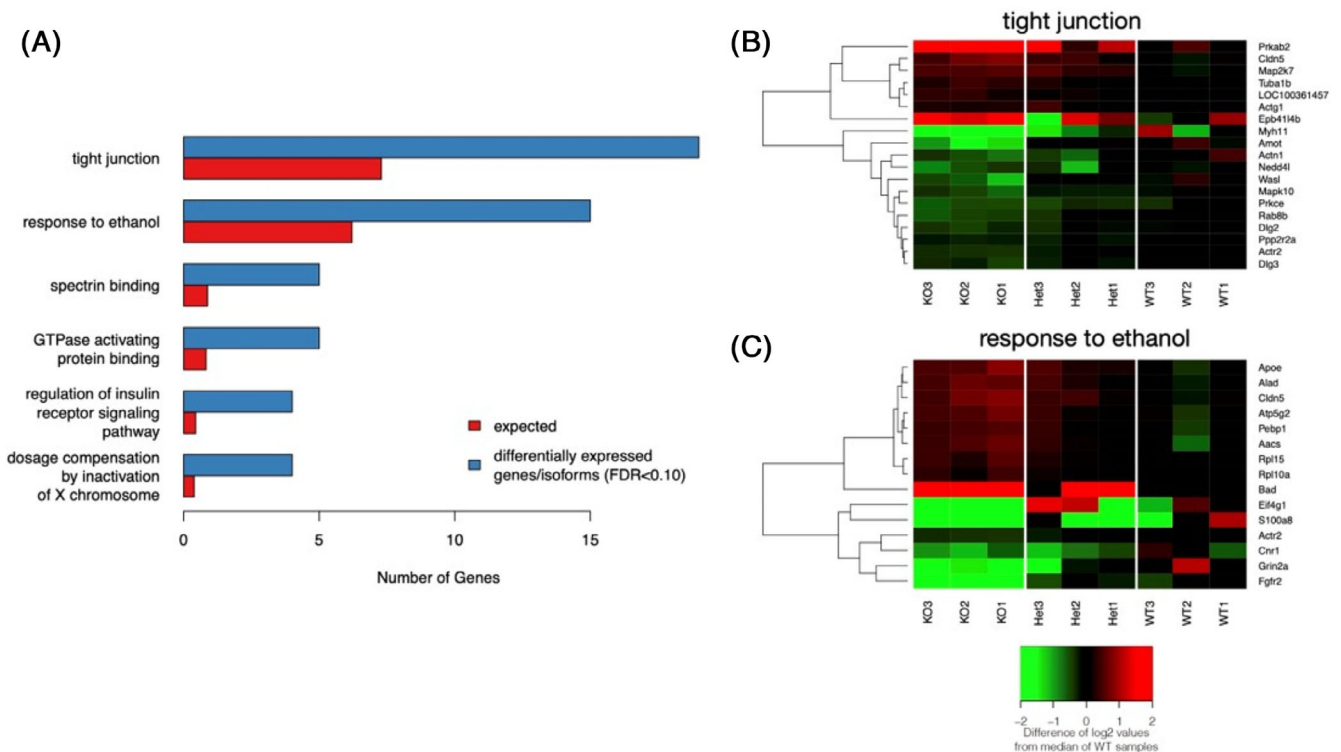


**FIGURE 4** Functional enrichment of KEGG pathways and Gene Ontology (GO) terms in transcripts differentially expressed between *Lrap* knockout and wild type rat brains. Genes associated with isoforms and/or SOI that were differentially expressed (FDR  $< 0.10$ ) were included. The background data set for enrichment include genes with at least one isoform and/or SOI that was expressed in brain and tested for differential expression. (A) Terms and pathways enriched for isoforms/SOI whose expression levels were altered by the genetic manipulation of *Lrap*. All pathways/terms included in the figure: (1) contained 3 or more differentially expressed isoform/SOI, (2) meet a significance threshold of an FDR  $< 0.10$ , and (3) had a fold enrichment (observed number of differentially expressed genes divided by the number of differentially expressed genes expected by chance) of at least 2. Fifteen GO terms met all three criteria but only the top 5 (by  $p$  value) are included in the graphic for simplicity. Differentially expressed isoforms/SOI associated with the (B) Tight Junction KEGG pathway or associated with the (C) Response to Ethanol GO term. Expression values are represented in this heatmap as the difference in  $\log_2$  transformed and library size adjusted read counts for a sample and the median of this transformed read count in the wild type rats

**TABLE 3** Possible mediators of the effect of Lrap on alcohol consumption

Gene symbol	Gene description	Physical location (RN6)	Correlation with alcohol consumption HXB/BXH RI Panel (microarrays)		Correlation with Lrap expression in HXB/BXH RI panel (microarrays)		eQTL in HXB/BXH RI panel (microarrays)	SOI-level analysis of Lrap <sup>-/-</sup> vs Lrap <sup>+/+</sup> (RNA-Seq)		SOI-level analysis of Lrap <sup>+/-</sup> vs Lrap <sup>-/-</sup> (RNA-Seq)		Combination of Lrap and alcohol consumption in the HXB/BXH and differential expression in Lrap <sup>-/-</sup> and Lrap <sup>+/+</sup>
			Correlation Coefficient (p value)	Correlation Coefficient (p value)	Position (95% Bayesian credible interval)	Genome-wide p value		Ratio of KO to WT	Unadjusted p value	Ratio of HET to WT	Unadjusted p value	
Cndp1	carnosine dipeptidase 1	Chr18: 81.5 Mb	0.63 (0.002)	-0.51 (0.0193)	Chr6: 6.6 Mb [3.6 to 145.8]	0.21	1.77	0.036	1.38	0.032	1.7E-06	9.5E-04
Ninj2	ninjurin 2	Chr4: 152.6 Mb	0.53 (0.012)	-0.63 (0.0024)	Chr4: 166.1 Mb [136.6 to 166.1]	0.025	1.3	0.045	1.06	0.411	1.3E-06	9.5E-04
P2rx4	purinergic receptor P2X 4	Chr12: 39.3 Mb	-0.63 (0.002)	0.84 (<0.0001)	Chr12: 39.1 Mb [39.1 to 41.5]	0.034	0.7	0.006	0.67	0.003	3.3E-11	2.9E-07
Slc35c2	solute carrier family 35 member C2	Chr3: 161.8 Mb	-0.57 (0.008)	0.53 (0.0142)	Chr17: 61.9 Mb [2.3 to 89.6]	0.375	1.47	0.001	1.44	0.002	1.4E-07	2.4E-04
Zfr2	zinc finger RNA binding protein 2	Chr7: 11.3 Mb	0.46 (0.035)	-0.46 (0.0364)	Chr9: 117.7 Mb [15.3 to 120]	0.232	1.38	0.028	1.14	0.229	3.6E-05	4.2E-03
Znhit6	zinc finger, HIT-type containing 6	Chr2: 251.5 Mb	-0.48 (0.028)	0.51 (0.0174)	Chr2: 251 Mb [146.8 to 259.9]	0.409	0.64	0.009	0.92	0.972	4.3E-06	1.7E-03

Note: Sums of isoforms (SOI) are included if they were correlated with alcohol consumption in the HXB/BXH recombinant inbred rat panel using the microarray data (unadjusted  $p$  value<0.05), correlated with Lrap in the HXB/BXH RI panel (unadjusted  $p$  value<0.05), and differentially expressed between the Lrap<sup>-/-</sup> and the wild type Lrap<sup>+/+</sup> rat in the RNASeq study (unadjusted  $p$  value<0.05).

Lrap, but not all of these are necessarily associated with, or determinants of, the level of alcohol consumption. To focus on Lrap-influenced transcripts that are likely to contribute to the relationship between Lrap and alcohol consumption, we combined gene expression information from the Lrap<sup>-/-</sup> RNASeq experiment and our original data that included Affymetrix Exon Array brain expression data and alcohol consumption measures from the HXB/BXH RI rat strains.<sup>14</sup> Of the 14,114 protein coding Ensembl genes (representing 33,063 isoforms) that were expressed above background in the RNASeq experiment, 8770 were also represented as expressed transcripts in the microarray experiment. We used a multi-level statistical strategy to arrive at association between gene product and phenotype. Of the 8770, the expression levels of 209 were significantly (unadjusted *p* < 0.05) correlated with alcohol consumption in the

HXB/BXH RI panel. Furthermore, 59 of those transcripts were also significantly correlated with Lrap expression in the HXB/BXH RI panel (unadjusted *p* value < 0.05). Finally, of the 59 transcripts correlated with both alcohol consumption and Lrap expression in the HXB/BXH RI panel, 6 had an SOI that was also differentially expressed within the RNASeq data (unadjusted *p* value < 0.05) between Lrap<sup>-/-</sup> and Lrap<sup>+/+</sup> rats (Table 3). All six are differentially expressed in the direction predicted from the correlation with Lrap in the microarray experiment, i.e., a positive correlation between the transcript and Lrap in the microarray experiment results in an expression ratio less than 1 for the comparison of Lrap<sup>-/-</sup> to Lrap<sup>+/+</sup>. To arrive at the identity of the six genes considered to be associated with both Lrap function and alcohol consumption, these candidates had to traverse three levels of statistical scrutiny (i.e., correlated with alcohol consumption across



FIGURE 5 Legend on next page.

HXB/BXH RI panel, expression correlated with *Lrap* expression across the HXB/BXH RI panel, and differentially expressed between *Lrap*<sup>+/+</sup> and *Lrap*<sup>-/-</sup> rats).

### 3.8 | *Lrap* characteristics and similarities with mouse and human sequences

A cross-species comparison for *Lrap* generated information that a similar transcript exists in the mouse, and the mouse DNA sequence producing this transcript (A930024E05Rik) resides in a region syntenic to the rat genome coding for *Lrap*. Certain regions of the DNA sequences for *Lrap* and A930024E05Rik have high homology. Particularly evident is the homology between the areas coding for what can be described as exon 1 in both species, as well as the region that was deleted in the *Lrap*<sup>-/-</sup> rats (Figure 5). It should be noted that in the rats, the deleted DNA region appears in an area characteristic of an exon. In the mouse, the homologous region starts within an exon sequence but a portion of the sequence of this homologous region is beyond a canonical splice signal sequence. The deletion would disrupt a splicing signal that would be necessary for linking Exon 2 and 3 in the mouse. It should also be noted that the sequences for *Lrap* in mouse and rat are on opposite strands (sense for mouse and antisense

for rat). In human, an *Lrap*-like sequence (AC145422.1) is evident in a DNA region that is syntenic with both mouse and rat *Lrap*-like regions and lies on the sense strand in this region. The current annotation of transcripts produced from this region of the human DNA indicates the presence of a transcript generated from two exons, with these exons being separated by a long (12,169 bp) intronic region (Figure 5A). The region homologous to the region that we deleted in the rat genome maps to the intronic region in the human. On closer examination, however, and using long polyA- RNA-Seq data from the ENCODE project on the GM12878 cell line, we noted that the region of the human DNA homologous to the area that we deleted in the rat produced RNA reads that could represent the presence of an unannotated exon of the human ortholog of *Lrap* being transcribed in the region identified as AC14522.1 (Figure 5E).

## 4 | DISCUSSION

It was by serendipity (and a false premise) that we chose the region to delete in *Lrap* to produce the *Lrap*<sup>-/-</sup> rats. The deleted region resembled an open reading frame (ORF) in the BN rat reference DNA, but the current comparison across species indicated that this is not an ORF in either mouse or human. Although the region resembling the

**FIGURE 5** Regions of the mouse and human genome homologous to the region of the rat genome that contains *Lrap*. The entire genomic sequence of *Lrap*, that is, including introns, from the rat was compared with the mouse genome and the human genome. (A) Alignment of the *Lrap* genomic sequence to the human genome. The green blocks in the first track denote areas of homology in the human DNA sequence. The numeric label on each box corresponds to a row in (F). The intensity of the green color is related to the percent identity of the two sequences. The area highlighted in gray designates the homologous region of the human genome that was deleted in the rat. The second track 'GENCODE v29 Comprehensive Transcript Set (+ only)' contains an annotated human transcript, AC145422.1, produced from the same strand that is homologous to the *Lrap* sequence in this region. (B) Alignment of the *Lrap* genomic sequence to the mouse genome. The green blocks in the first track denote areas of homology in the mouse DNA sequence. The numeric label on each box corresponds to a row in (G). The intensity of the green color is related to the percent identity of the two sequences. The area highlighted in gray designates the homologous region of the mouse genome that was deleted in the rat. The second track 'GENCODE VM20 Comprehensive Transcript Set (+ only)' contains an annotated mouse transcript, A930024E05Rik, produced from the same strand that is homologous to the *Lrap* sequence in this region. (C) Human and mouse homologous sequences mapped onto the rat genome. The first track, 'Human Alignment', highlights the regions of the rat genome that are homologous to the human genome using the same coloring and labeling as in (A). The second track, 'Mouse Alignment', highlights the regions of the rat genome that are homologous to the mouse genome using the same coloring and labeling as in (B). The third track, '*Lrap*', contains the original structure of *Lrap* derived from the transcriptome reconstruction in the SHR and BN-Lx brain RNASeq data in blue and the region of *Lrap* that was eliminated in the knockout rats in red. Please note that the homologous regions have been superimposed and intervening regions are not to the same scale. In addition, since *Lrap* was transcribed from the negative strand in rat but is homologous to regions on the positive strand in both human and mouse, the orientation of (C) has been flipped so that the first exon of *Lrap* is on the left and the last exon of *Lrap* is on the right. (D) Genetic variants within the genomic area of *Lrap*. This panel provides information on polymorphisms (SNPs and indels) distinguishing the Wistar Kyoto rat strain and the related SHR rat strain from the BN rat strain (reference strain). This illustration also indicates the indels and SNPs that disrupt the possible ORF in the BN sequence. (E) RNA expression in human of *Lrap* locus. The genomic area depicted in this panel covers chr12:121,579,800–121,593,949 bp of the human genome (hg38). The first track 'GENCODE v29 Comprehensive Transcript Set (+ only)' contains an annotated human transcript, AC145422.1, produced from the plus strand. The second track 'LRAP (WKY rn6) alignment to Human' includes regions of human genome that are homologous to the region of the rat genome that produces the *Lrap* transcript. The intensity of the green color is related to the percent identity of the two sequences. The area highlighted in gray designates the homologous region of the human genome that was deleted in the rat. The third and final track 'GM12878 ENCODE/CSHL PolyA- (+ strand)' indicates the number of RNASeq reads that align to the region. RNASeq reads generated by the ENCODE/Cold Spring Harbor Lab were derived from long polyA- sequence of the GM12878 cell line and are publicly available through the UCSC Genome Browser and through the Gene Omnibus Database (GEO Accession: GSM758572). (F) Summary of *Lrap* alignment to the human genome contains additional detail, including percent homology, about the alignment of *Lrap* to the human genome. The numeric labels on the rows correspond to the green blocks in (A) with the same label. (G) Summary of *Lrap* alignment to the mouse genome contains additional detail, including percent homology, about the alignment of *Lrap* to the mouse genome. The numeric labels on the rows correspond to the green blocks in (B) with the same label

ORF in rat, appears as an ORF in the reference BN genome, in other strains of rats, and particularly Wistar-derived strains, the putative ORF is disrupted by an indel and SNPs (shown in Figure 5 for Wistar-derived strains). The Wistar strain was used to generate our  $Lrap^{-/-}$  and  $Lrap^{+/-}$  rats. The maintenance of sequences homologous (but not identical) to the deleted region in species from mouse to human may indicate that the deleted region in the rat DNA, even though it is not apt to be translated, still has a functional significance. Since our genetic manipulation of *Lrap* produced a lesser reduction of the expression of other segments of *Lrap* (e.g., Exons 1 and 2), one might conclude that the excised sequence is an important component of the mechanism of action of *Lrap*. However, we do note the possibility that the decrease in levels of exons 1 and 2 in the  $Lrap^{-/-}$  rat could also contribute to the observed results.

We had previously postulated that the disruption of *Lrap* would result in increased alcohol consumption, based on our prior finding of a negative correlation between alcohol consumption and brain *Lrap* levels across the rat HXB/BXH RI panel.<sup>14</sup> Our results with the Wistar rats in which *Lrap* was disrupted confirmed this hypothesis, showing that alcohol consumption was doubled in  $Lrap^{-/-}$  rats, and increased by 50% in the  $Lrap^{+/-}$  animals, when compared with the  $Lrap^{+/+}$  rats. When we calculated an alcohol preference ratio (volume of 10% alcohol solution/total volume of fluid consumed/day), we noted a similar order, with the  $Lrap^{-/-}$  rats displaying the highest preference ratio. We also noted that the constitutive deletion of this portion of *Lrap* altered the expression of transcripts of 750 protein-coding genes in brain when comparing adult  $Lrap^{+/+}$  and  $Lrap^{-/-}$  rats. When considering a change in the levels of such a number of transcripts by deletion of a segment of a lncRNA in our studies, one is drawn to consider functions of lncRNA that are more global than discrete (i.e., acting on transcription or stability of a particular transcript or a small number of transcripts).<sup>39</sup> Two more global functions that have been described for lncRNA, are chromatin structure modification through interaction with histones<sup>40</sup> and modulation of alternative splicing.<sup>41</sup> By examining the effect of knockdown of 39 lncRNAs in three human cell lines, Wendt Porto et al.<sup>41</sup> identified 17,525 alternative splicing events. Many of these events were cell-specific and were a result of lncRNA-induced alternative splicing related to RNA binding protein pre-mRNA interactions at splice junctions.<sup>41</sup> Another mechanism by which lncRNA can produce large scale changes in splicing is by modulating the phosphorylation of splicing factors or by direct interactions "hijacking" splicing factors.<sup>4</sup> The pattern (isoform level changes) and extent of changes we noted in protein-coding transcripts (i.e., 708 of the 782 differentially expressed isoforms did not have corresponding changes at the SOI level) may well indicate that *Lrap* is a lncRNA that has as its major function, the modulation of alternative splicing. That is, the genetic deletion of a portion of *Lrap* primarily changed the quantitative relationship between the isoforms derived from a particular gene, rather than the total quantity of transcripts generated from a gene. We also examined more thoroughly the character of differences in splicing events (as opposed to quantitative differences in isoform expression levels) occurring between the  $Lrap^{+/+}$  and  $Lrap^{-/-}$  rats. The rMATS algorithm distinguishes between five types of alternative

splicing events and can indicate the differential presence of an isoform produced from a particular gene across experimental conditions compared. Within the 601 differentially expressed isoforms analyzed with the rMATS algorithm, 133 isoforms were predominantly unique to either  $Lrap^{+/+}$  or  $Lrap^{-/-}$  rats. In other words, these isoforms were specifically expressed in either  $Lrap^{+/+}$  and  $Lrap^{-/-}$  strains. This would indicate that *Lrap* can change both quantitative and qualitative characteristics of splicing.

On the other hand, the total quantity of transcript derived from the gene *P2rx4* was significantly different between  $Lrap^{+/+}$  and  $Lrap^{-/-}$  rats, but the ratio of the two isoforms of this gene remained constant. It was of interest that *P2rx4* was the one gene product in the module in which *Lrap* was designated as the "hub" gene ("most connected") that was significantly changed in its level of expression in brain between  $Lrap^{+/+}$  and  $Lrap^{-/-}$  rats. In addition, its expression level was significantly correlated with levels of *Lrap* expression across the HxB/BxH panel of recombinant inbred rat strains. One needs to be cognizant that the coexpression relationships that determine segregation of transcripts into a module when using WGCNA,<sup>16</sup> do not necessarily indicate that the transcripts included within a module have an identical form of co-regulation,<sup>42</sup> and coexpression may be a result of coordinated responses, through different mechanisms, to a particular cellular state or signal.

However, the significant correlation between *Lrap* expression and the total levels of *P2rx4* expression, as well as *P2rx4* expression and alcohol consumption, bears some additional attention. *P2rx4* is a ligand-gated calcium channel activated by ATP,<sup>43</sup> and its function has been linked by numerous studies to control of alcohol consumption in rats and mice.<sup>44-47</sup> Many lncRNAs are expressed in a tissue and/or cell-specific manner,<sup>8,48</sup> and one could invoke a "guilt by association" approach<sup>49</sup> to hypothesize in which brain cells *Lrap* is directly influencing the expression of other transcripts. The high correlation of *Lrap* expression with expression of *P2rx4* could indicate that these two transcripts may be localized to the same cell type. *P2rx4* shows a broad distribution in the CNS and is present in both neurons and glial cells.<sup>49</sup> Data generated by Dong et al<sup>50</sup> indicate that the expression of the *Lrap* homolog (A930024E05Rik) in adolescent (P17) mice is highest in microglia compared with other cell types in brain, and thus a relationship between *Lrap* and *P2rx4* expression may be most evident in microglia. Microglia are ubiquitous throughout the brain and if *Lrap* is localized to microglia, the distribution of the *Lrap* mouse homolog A930024E05Rik noted in the Allen Mouse Brain Atlas would be instructive.<sup>51</sup> The Allen Brain Atlas shows that *Lrap* appears at low levels throughout the adult mouse brain and resembles the expected distribution of microglia. It is of interest that our original interpretation of the function of the co-expressed components of the module, for which *Lrap* was the hub gene, led us to conclude that the components of the module were related to "immune function, energy metabolism, calcium homeostasis and glial-neuronal communication".<sup>14</sup>

Furthermore, we examined the expression values for *Lrap* in liver tissue from the BN-Lx/Cub and SHR/OlaIpcv that we assayed using RNA-Seq in a manner similar to the methods used here.<sup>52</sup> There was evidence for *Lrap* expression in both read coverage and coverage of



specific exon junctions of *Lrap* (<http://phenogen.org>). There was also evidence of expression of the mouse homolog from the Expression Atlas<sup>53</sup> in the Ensembl database (<http://ensembl.org>) across several tissues including liver, lung, spleen, colon, heart, and kidney and across several brain regions with the highest expression in brain and testis. For the human homolog, we examined data from GTEx<sup>54</sup> available through the UCSC genome browser.<sup>37</sup> Similar to mouse, this transcript was expressed across many tissue tissues with the highest expression in testis and brain. Further research is needed to fully understand the relationship of expression of *Lrap* in different tissues with alcohol consumption and other phenotypes.

As stated above, our RNASeq studies of the adult brain transcriptome indicated extensive changes in gene expression between *Lrap*<sup>+/+</sup> and *Lrap*<sup>-/-</sup> rats. When the genes with an isoform or a SOI that was differentially expressed in brains of adult *Lrap*<sup>+/+</sup> and *Lrap*<sup>-/-</sup> rats were subjected to functional enrichment analysis using GO or KEGG, the most significant pathway using KEGG, was "Tight Junction". In the CNS, tight junctions are evident between astrocytes and oligodendrocytes and capillary endothelial cells, as well as between glia and axons and in the myelin sheath.<sup>55-57</sup> The Tight Junction category encompasses MAGUK (zonula occludens, ZO) tight junction-associated proteins that participate in signal transduction at specialized cell-cell junctions<sup>58</sup> and claudin 5, which is an essential functional component of endothelial tight junctions.<sup>59</sup> Current evidence shows that microglia participate in the integrity of the endothelial tight junction and modulation of microglial phenotype can alter brain endothelial permeability.<sup>60</sup> It is becoming evident that changes in endothelial permeability and increased entry of pattern recognition receptor ligands into brain, with generation of inflammatory responses, may contribute to increases in alcohol consumption by rodents<sup>61</sup> and possibly humans.<sup>62</sup>

Among the top 5 GO terms that met our requirements for significance in enrichment (Figure 4A), transcripts in two of the five categories could be linked to receptor signaling (GTPase activating protein binding, regulation of insulin receptor signaling pathway) and one to neuronal membrane integrity (spectrin binding), while transcripts in one category were associated with X chromosome inactivation. X-chromosome inactivation is a well-studied epigenetic phenomenon associated with many lncRNA.<sup>63</sup> The last of these significantly enriched GO terms was "Response to Alcohol". In this category were several isoforms of *Actr2*, actin related protein (ARP) homologs (with isoforms recognized through our RNASeq transcriptome reconstruction) and *claudin 5*, which was also part of the "Tight Junction" pathway in KEGG. The ARP is important in early synaptogenesis.<sup>64</sup> Two neurotransmitter receptor transcripts were also evident in the GO "Response to Alcohol" category: *Cnr1* (cannabinoid receptor 1; CB1) and *Grin2a* (the GluN2A subunit of the NMDA receptor). The CB1 receptor has been linked to control of alcohol consumption in mice<sup>65</sup> and the NMDA receptor has been linked to alcohol tolerance and the hyperexcitability seen on withdrawal in alcohol-dependent animals, including humans.<sup>66</sup>

As attractive as it may seem to associate individual gene products that are differentially expressed between *Lrap*<sup>+/+</sup> and *Lrap*<sup>-/-</sup> rats to differences in alcohol consumption, based on their function or inclusion in a particular GO category or KEGG pathway, one needs to, at

least, consider that a candidate transcript should also be quantitatively related to the phenotype of interest. This assumption of quantitative genetics could be tested in our HXB/BXH RI panel of rats by measuring the correlation between levels of transcript expression and the phenotype of alcohol consumption (g/kg). Our analysis identified the products of six genes (*Cndp1*, *Ninj2*, *P2rx4*, *Slc35c2*, *Zfr2* and *Znhit6*) that were differentially expressed between the *Lrap*<sup>-/-</sup> and *Lrap*<sup>+/+</sup> rats, and correlated in their expression levels with both *Lrap* expression and alcohol consumption across the panel of HXB/BXH RI rat strains (Table 3). Based on the statistical significance of the various correlations and comparisons, *P2rx4* stood out as the best candidate fulfilling all criteria, and its relationship to alcohol consumption was mentioned earlier. The functions of the other gene products can be related to neurological disorders, neurogenesis, inflammation/immune regulation and transcriptional activity.<sup>67-75</sup> These gene products may be considered as additional factors contributing to the phenotypes of alcohol consumption and/or alcohol preference in rats.

It should be noted that our experimental design is focused on ascertaining genetic components that generate a predisposition to particular phenotypes (i.e., predisposition to consumption of alcohol in the initial stages of exposure, not alcohol dependence).<sup>14</sup> Thus, our measures of gene expression and analysis of coexpression modules and networks takes place in animals not exposed to ethanol. We then measure alcohol consumption in another cohort from the same strains of rats, presuming that the gene expression patterns will remain constant in rats which are isogenic within a strain and are raised in an identical environment. The genetic differences between strains are considered to contribute to differences in gene expression and the subsequent differences in alcohol drinking and/or other phenotypes. Another caveat that needs to be noted, is that our studies were performed using male rats. The importance of lncRNAs in X chromosome inactivation and epigenetic programming would predicate that similar experiments be performed in female animals.

We have established the presence of a novel lncRNA in rat brain (*Lrap*) and produced evidence that homologous transcripts can be produced from syntenic regions of the genome of mice and humans. We have provided evidence of a significant negative correlation between *Lrap* expression and expression of *P2rx4* in adult brain, and a significant correlation between both of these transcripts (*Lrap* and *P2rx4*) and levels of alcohol consumption across 21 strains of rats within a RI panel of rats (HXB/BXH). By disrupting a specific area of *Lrap* (an area also present in the genome of both mouse and human), we show that predicted changes (based on prior correlation analysis) take place in both the expression of *P2rx4* and alcohol consumption when comparing the rats with the disrupted *Lrap* sequence and the *Lrap*<sup>+/+</sup> controls. This information focuses attention on a region of the sequence of *Lrap* that may have functional implications. In addition, we show that constitutive disruption of *Lrap* produces broad based changes in the brain transcriptome, and show that *Lrap* effects are most evident in terms of alternative splicing of a large number of transcripts. Our results suggest that *Lrap* may be an important component controlling isoform expression, and that a subset of the genes whose expression is influenced by disruption of *Lrap* is predisposing the phenotype of

elevated alcohol consumption. An important caveat is that our studies have been performed in male animals and extrapolation to females requires further work.

## ACKNOWLEDGMENTS

The authors sincerely thank Carolyn Ferguson and Matthew McKay for help in the generation of the genetically modified rats, Seija Tillanen for assistance in the molecular biology experiments and Yinni Yu for help with the animal drinking studies. They would also like to thank the Integrative Neuroscience Initiative on Alcoholism-Neuroimmune for their continued support and encouragement.

## DATA AVAILABILITY

The data that support the findings of this study are openly available in Gene Expression Omnibus database at <https://www.ncbi.nlm.nih.gov/geo/>, reference number GSE1557079.

## ORCID

Boris Tabakoff  <https://orcid.org/0000-0001-5132-5030>

## REFERENCES

- Ernst C, Morton CC. Identification and function of long non-coding RNA. *Front Cell Neurosci.* 2013;7:168.
- Sun Q, Hao Q, Prasanth KV. Nuclear Long noncoding RNAs: key regulators of gene expression. *Trends Genet.* 2018;34(2):142-157.
- Vance KW, Ponting CP. Transcriptional regulatory functions of nuclear long noncoding RNAs. *Trends Genet.* 2014;30(8):348-355.
- Romero-Barrios N, Legascue MF, Benhamed M, Ariel F, Crespi M. Splicing regulation by long noncoding RNAs. *Nucleic Acids Res.* 2018;46(5):2169-2184.
- Long Y, Wang X, Youmans DT, Cech TR. How do lncRNAs regulate transcription? *Sci Adv.* 2017;3:eaa02110.
- Clark BS, Blackshaw S. Understanding the role of lncRNAs in nervous system development. *Adv Exp Med Biol.* 2017;1008:253-282.
- Pereira Fernandes D, Bitar M, Jacobs FMJ, Barry G. Long non-coding RNAs in neuronal aging. *Noncoding RNA.* 2018;4(2):12.
- Derrien T, Johnson R, Bussotti G, et al. The GENCODE v7 catalog of human long noncoding RNAs: analysis of their gene structure, evolution, and expression. *Genome Res.* 2012;22(9):1775-1789.
- Wang A, Wang J, Liu Y, Zhou Y. Mechanisms of Long non-coding RNAs in the assembly and plasticity of neural circuitry. *Front Neural Circuits.* 2017;11:76.
- Fochler S, Morozova TV, Davis MR, et al. Genetics of alcohol consumption in *Drosophila melanogaster*. *Genes Brain Behav.* 2017;16(7):675-685.
- Leggio L, Addolorato G, Cipitelli A, Jerlhag E, Kampov-Polevoy AB, Swift RM. Role of feeding-related pathways in alcohol dependence: a focus on sweet preference, NPY, and ghrelin. *Alcohol Clin Exp Res.* 2011;35(2):194-202.
- Brasser SM, Castro N, Feretic B. Alcohol sensory processing and its relevance for ingestion. *Physiol Behav.* 2015;148:65-70.
- Clarke TK, Adams MJ, Davies G, et al. Genome-wide association study of alcohol consumption and genetic overlap with other health-related traits in UKbiobank (N=112 117). *Mol Psychiatry.* 2017;22(10):1376-1384.
- Saba LM, Flink SC, Vanderlinden LA, et al. The sequenced rat brain transcriptome—its use in identifying networks predisposing alcohol consumption. *FEBS J.* 2015;282(18):3556-3578.
- Doss S, Schadt EE, Drake TA, Lusis AJ. Cis-acting expression quantitative trait loci in mice. *Genome Res.* 2005;15(5):681-691.
- Langfelder P, Horvath S. WGCNA: an R package for weighted correlation network analysis. *BMC Bioinform.* 2008;9:559.
- Mulligan MK, Abreo T, Neuner SM, et al. Identification of a functional non-coding variant in the GABA<sub>A</sub> receptor alpha2 subunit of the C57BL/6J mouse reference genome: major implications for neuroscience research. *Front Genet.* 2019;10:188.
- Blednov YA, Borghese CM, Ruiz CI, et al. Mutation of the inhibitory ethanol site in GABA<sub>A</sub> rho1 receptors promotes tolerance to ethanol-induced motor incoordination. *Neuropharmacology.* 2017;123:201-209.
- Hsu PD, Scott DA, Weinstein JA, et al. DNA targeting specificity of RNA-guided Cas9 nucleases. *Nat Biotechnol.* 2013;31(9):827-832.
- Bassett AR, Tibbit C, Ponting CP, Liu JL. Highly efficient targeted mutagenesis of drosophila with the CRISPR/Cas9 system. *Cell Rep.* 2014;6(6):1178-1179.
- Cong L, Ran FA, Cox D, et al. Multiplex genome engineering using CRISPR/Cas systems. *Science.* 2013;339(6121):819-823.
- Zhou Z, Karlsson C, Liang T, et al. Loss of metabotropic glutamate receptor 2 escalates alcohol consumption. *Proc Natl Acad Sci U S A.* 2013;110(42):16963-16968.
- Tabakoff B, Saba L, Printz M, et al. Genetical genomic determinants of alcohol consumption in rats and humans. *BMC Biol.* 2009;7:70.
- Martin MW. Cutadapt removes adapter sequences from high-throughput sequencing reads. *EMBnet. journal.* 2011;17:10-12.
- Kim D, Paggi JM, Park C, Bennett C, Salzberg SL. Graph-based genome alignment and genotyping with HISAT2 and HISAT-genotype. *Nature Biotechnology.* 2019;37:907-915.
- Pertea M, Pertea GM, Antonescu CM, Chang TC, Mendell JT, Salzberg SL. StringTie enables improved reconstruction of a transcriptome from RNA-seq reads. *Nat Biotechnol.* 2015;33(3):290-295.
- Pertea M, Kim D, Pertea GM, Leek JT, Salzberg SL. Transcript-level expression analysis of RNA-seq experiments with HISAT, StringTie and Ballgown. *Nat Protoc.* 2016;11(9):1650-1667.
- Parikhshak NN, Swarup V, Belgard TG, et al. Genome-wide changes in lncRNA, splicing, and regional gene expression patterns in autism. *Nature.* 2016;540(7633):423-427.
- Li B, Dewey CN. RSEM: accurate transcript quantification from RNA-Seq data with or without a reference genome. *BMC Bioinform.* 2011;12:323.
- Love MI, Huber W, Anders S. Moderated estimation of fold change and dispersion for RNA-seq data with DESeq2. *Genome Biol.* 2014;15(12):550.
- Benjamini Y, Hochberg Y. Controlling the false discovery rate: a practical and powerful approach to multiple testing. *J R Stat Soc Ser B.* 1995;57:289-300.
- Kanehisa M, Furumichi M, Tanabe M, Sato Y, Morishima K. KEGG: new perspectives on genomes, pathways, diseases and drugs. *Nucleic Acids Res.* 2017;45(D1):D353-D361.
- Consortium TGO. The gene ontology resource: 20 years and still GOing strong. *Nucleic Acids Res.* 2019;47(D1):D330-D338.
- Durinck S, Spellman PT, Birney E, Huber W. Mapping identifiers for the integration of genomic datasets with the R/bioconductor package biomaRt. *Nat Protoc.* 2009;4(8):1184-1191.
- Shen S, Park JW, Lu Z, Lin L, Henry MD, Wu YN, Zhou Q, Xing Y. rMATS: Robust and flexible detection of differential alternative splicing from replicate RNA-Seq data. *PNAS.* 2014;111:E5593-E5601.
- Hermesen R, de Ligt J, Spee W, et al. Genomic landscape of rat strain and substrain variation. *BMC Genomics.* 2015;16:357.
- Kent WJ, Sugnet CW, Furey TS, et al. The human genome browser at UCSC. *Genome Res.* 2002;12(6):996-1006.
- Gonzalez I, Munita R, Agirre E, et al. A lncRNA regulates alternative splicing via establishment of a splicing-specific chromatin signature. *Nat Struct Mol Biol.* 2015;22(5):370-376.

39. Fernandes JCR, Acuna SM, Aoki JI, Floeter-Winter LM, Muxel SM. Long non-coding RNAs in the regulation of gene expression: physiology and disease. *Noncoding RNA*. 2019;5(1):17.
40. Khalil AM, Guttman M, Huarte M, et al. Many human large intergenic noncoding RNAs associate with chromatin-modifying complexes and affect gene expression. *Proc Natl Acad Sci U S A*. 2009;106(28):11667-11672.
41. Porto FW, Daulatabad SV, Janga SC. Long non-coding RNA expression levels modulate cell-type-specific splicing patterns by altering their interaction landscape with RNA-binding proteins. *Genes (Basel)*. 2019;10(8):593.
42. Zhang Y, Zha H, Wang JZ, Chu CH. Gene Co-regulation vs. Co-expression. Poster Proceedings of the International Conference on Research in Computational Molecular Biology (RECOMB), San Diego, CA; 2004. pp. 232-233.
43. Stokes L, Layhadi JA, Bibic L, Dhuna K, Fountain SJ. P2X4 receptor function in the nervous system and current breakthroughs in pharmacology. *Front Pharmacol*. 2017;8:291.
44. Wyatt LR, Finn DA, Khoja S, et al. Contribution of P2X4 receptors to ethanol intake in male C57BL/6 mice. *Neurochem Res*. 2014;39(6):1127-1139.
45. Franklin KM, Asatryan L, Jakowec MW, Trudell JR, Bell RL, Davies DL. P2X4 receptors (P2X4Rs) represent a novel target for the development of drugs to prevent and/or treat alcohol use disorders. *Front Neurosci*. 2014;8:176.
46. Khoja S, Huynh N, Asatryan L, Jakowec MW, Davies DL. Reduced expression of purinergic P2X4 receptors increases voluntary ethanol intake in C57BL/6J mice. *Alcohol*. 2018;68:63-70.
47. Franklin KM, Hauser SR, Lasek AW, Bell RL, McBride WJ. Involvement of Purinergic P2X4 receptors in alcohol intake of high-alcohol-drinking (HAD) rats. *Alcohol Clin Exp Res*. 2015;39(10):2022-2031.
48. Quinn JJ, Chang HY. Unique features of long non-coding RNA biogenesis and function. *Nat Rev Genet*. 2016;17(1):47-62.
49. Wolfe CJ, Kohane IS, Butte AJ. Systematic survey reveals general applicability of "guilt-by-association" within gene coexpression networks. *BMC Bioinform*. 2005;6:227.
50. Dong X, Chen K, Cuevas-Diaz Duran R, et al. Comprehensive identification of Long non-coding RNAs in purified cell types from the brain reveals functional lncRNA in OPC fate determination. *PLoS Genet*. 2015;11(12):e1005669.
51. McCarthy M. Allen brain atlas maps 21,000 genes of the mouse brain. *Lancet Neurol*. 2006;5(11):907-908.
52. Harrall KK, Kechris KJ, Tabakoff B, et al. Uncovering the liver's role in immunity through RNA co-expression networks. *Mamm Genome*. 2016;27(9-10):469-484.
53. Papatheodorou I, Moreno P, Manning J, et al. Expression atlas update: from tissues to single cells. *Nucleic Acids Res*. 2020;48(D1):D77-D83.
54. Mele M, Ferreira PG, Reverter F, et al. Human genomics. The human transcriptome across tissues and individuals. *Science*. 2015;348(6235):660-665.
55. Abbott NJ, Ronnback L, Hansson E. Astrocyte-endothelial interactions at the blood-brain barrier. *Nat Rev Neurosci*. 2006;7(1):41-53.
56. Gonzalez-Mariscal L, Betanzos A, Nava P, Jaramillo BE. Tight junction proteins. *Prog Biophys Mol Biol*. 2003;81(1):1-44.
57. Niu J, Tsai HH, Hoi KK, et al. Aberrant oligodendroglial-vascular interactions disrupt the blood-brain barrier, triggering CNS inflammation. *Nat Neurosci*. 2019;22(5):709-718.
58. Gonzalez-Mariscal L, Betanzos A, Avila-Flores A. MAGUK proteins: structure and role in the tight junction. *Semin Cell Dev Biol*. 2000;11(4):315-324.
59. Van Itallie CM, Anderson JM. Claudin interactions in and out of the tight junction. *Tissue Barriers*. 2013;1(3):e25247.
60. Mehrbadi AR, Korolainen MA, Odero G, Miller DW, Kauppinen TM. Poly(ADP-ribose) polymerase-1 regulates microglia mediated decrease of endothelial tight junction integrity. *Neurochem Int*. 2017;108:266-271.
61. Mayfield J, Harris RA. The Neuroimmune basis of excessive alcohol consumption. *Neuropsychopharmacology*. 2017;42(1):376.
62. Warden A, Erickson E, Robinson G, Harris RA, Mayfield RD. The neuroimmune transcriptome and alcohol dependence: potential for targeted therapies. *Pharmacogenomics*. 2016;17(18):2081-2096.
63. Lee JT. Lessons from X-chromosome inactivation: long ncRNA as guides and tethers to the epigenome. *Genes Dev*. 2009;23(16):1831-1842.
64. Spence EF, Kanak DJ, Carlson BR, Soderling SH. The Arp2/3 complex is essential for distinct stages of spine synapse maturation, including synapse Unsilencing. *J Neurosci*. 2016;36(37):9696-9709.
65. Balla A, Dong B, Shilpa BM, et al. Cannabinoid-1 receptor neutral antagonist reduces binge-like alcohol consumption and alcohol-induced accumbal dopaminergic signaling. *Neuropharmacology*. 2018;131:200-208.
66. Krystal JH, Petrakis IL, Mason G, Trevisan L, D'Souza DC. N-methyl-D-aspartate glutamate receptors and alcoholism: reward, dependence, treatment, and vulnerability. *Pharmacol Ther*. 2003;99(1):79-94.
67. Babizhayev MA. Biochemical, biomedical and metabolic aspects of imidazole-containing dipeptides with the inherent complexity to neurodegenerative diseases and various states of mental well-being: a challenging correction and Neurotherapeutic pharmaceutical biotechnology for treating cognitive deficits, depression and intellectual disabilities. *Curr Pharm Biotechnol*. 2014;15(8):738-778.
68. Araki T, Milbrandt J. Ninjurin2, a novel homophilic adhesion molecule, is expressed in mature sensory and enteric neurons and promotes neurite outgrowth. *J Neurosci*. 2000;20(1):187-195.
69. Wang J, Fa J, Wang P, et al. NINJ2- a novel regulator of endothelial inflammation and activation. *Cell Signal*. 2017;35:231-241.
70. Lu L, Hou X, Shi S, Korner C, Stanley P. Slc35c2 promotes Notch1 fucosylation and is required for optimal notch signaling in mammalian cells. *J Biol Chem*. 2010;285(46):36245-36254.
71. Feng S, Shi T, Qiu J, et al. Notch1 deficiency in postnatal neural progenitor cells in the dentate gyrus leads to emotional and cognitive impairment. *FASEB J*. 2017;31(10):4347-4358.
72. He F, Umehara T, Tsuda K, et al. Solution structure of the zinc finger HIT domain in protein FON. *Protein Sci*. 2007;16(8):1577-1587.
73. Cloutier P, Poitras C, Durand M, et al. R2TP/Prefoldin-like component RUVBL1/RUVBL2 directly interacts with ZNHIT2 to regulate assembly of U5 small nuclear ribonucleoprotein. *Nat Commun*. 2017;8:15615.
74. Malinova A, Cvackova Z, Mateju D, et al. Assembly of the U5 snRNP component PRPF8 is controlled by the HSP90/R2TP chaperones. *J Cell Biol*. 2017;216(6):1579-1596.
75. Fu M, Blakeshear PJ. RNA-binding proteins in immune regulation: a focus on CCCH zinc finger proteins. *Nat Rev Immunol*. 2017;17(2):130-143.

## SUPPORTING INFORMATION

Additional supporting information may be found online in the Supporting Information section at the end of this article.

**How to cite this article:** Saba LM, Hoffman PL, Homanics GE, et al. A long non-coding RNA (Lrap) modulates brain gene expression and levels of alcohol consumption in rats. *Genes, Brain and Behavior*. 2021;20:e12698. <https://doi.org/10.1111/gbb.12698>